

**11th International**  
**Workshop on**  
**Semiconductor Oxides**

**Book of Abstracts**

## **Table of Contents**

<u>Title</u>	<u>Authors</u>	<u>Page</u>
<b>Day One</b>		
Advances in gallium oxide material and device technologies	Masataka Higashiwaki	7
CVD Diamond: Materials, Interfaces and Devices for Power, RF and Extreme Environments	Robert J. Nemanich	8
Low-PBTS defect-engineered high-mobility metal-oxide BEOL-compatible transistors	Milan Pešić	9
Advances in Ga <sub>2</sub> O <sub>3</sub> Power Device Development	Kohei Sasaki	10
Unconventional doping methods for Ga <sub>2</sub> O <sub>3</sub> and ZnO	Farida Selim	11
Origins and dynamic properties of midgap recombination centers in ZnO	S. F. Chichibu	12
Towards In Situ Visualization of Nanoscale and Atomic-Level Dynamics and Transport in Oxides	Peter Crozier	13
{ZnCdO/ZnMgO} SLs in situ Eu-doped growth by PA-MBE	E. Przeździecka	14
Ion irradiation induced phase transformation in $\beta$ -Ga <sub>2</sub> O <sub>3</sub> through in-situ ion irradiation in a TEM	Djamel Kaoumi	15
<b>Day Two</b>		
Growth and basic physical properties of bulk single crystals of transparent semiconducting oxides	Zbigniew Galazka	17
On the relationship between atomic and electronic structure on Ln-bearing oxides	Blas Pedro Uberuaga	18
Defect modeling and damage buildup in ion-bombarded oxides	Przemysław Jóźwik	19
Acceptor complexes in ZnO – effect of strain, surface proximity and carbon content	Elżbieta Guziewicz,	20
Persistent optical phenomena in oxide semiconductors	M.D. McCluskey	21

Positron Annihilation Spectroscopy (PAS) of PbO direct-photoconductor material deposited at low temperature for the development of TFT-based x-ray imaging	J.M. Gaudet	22
Photoluminescence of spinel MgGa <sub>2</sub> O <sub>4</sub> and ZnGa <sub>2</sub> O <sub>4</sub> thin films grown by molecular beam epitaxy	Jianlin Liu	23
Internal and External Control of Excitons in Colloidal Quantum Dots	J. A. Hollingsworth	24
Electric Field Engineering to Unlock the Potential of Gallium Oxide Power Devices	Nolan Hendricks	25
Study on Metal-Oxide Field Effect Transistors of $\beta$ -Gallium Oxide with AlGaO Spacer Layer for High Power Device Applications	Sheng-Ti Chung	26
Computational design of optimal heterostructure materials for monoclinic Ga <sub>2</sub> O <sub>3</sub>	Hartwin Peelaers	27
Combinatorial Synthesis and Physical Property Screening of Ternary Alloys of Rhombohedral $\alpha$ -Ga <sub>2</sub> O <sub>3</sub> and Transition Metal Sesquioxides	Clemens Petersen	28
Metal-Semiconductor Interfaces and Ohmic Contacts on $\beta$ -Ga <sub>2</sub> O <sub>3</sub>	Kathleen T. Smith	29
Ion Beam Synthesis of Layer-Tunable and Transfer Free Graphene for Device Applications	Yongqiang Wang	30
Study of interfacial properties of Ti/ Ga <sub>2</sub> O <sub>3</sub> Schottky junctions processed with SiH <sub>4</sub> plasma	Sahyadri Patil, Mengbing Huang	31
<b>Day Three</b>		
Formation of strain relaxed thin (<30nm) epitaxial Si <sub>1-x</sub> Gex layers on a silicon substrate via ion implantation and selective oxidation	Andrew P. Knights	33
Cryogenic Performance of In <sub>0.8</sub> Ga <sub>0.2</sub> As Quantum-Well HEMTs: Scaling Limits and High-Frequency Operation	Tae-Woo Kim	34
Visualization of polarization induced phonons in	Sandhya Susarla	35

## ferroelectric oxides

Transparent Hybrid Electrodes for Next-Generation Flexible Photovoltaic Applications	Terry Alford	36
Correlations between the growth conditions of homoepitaxially grown $\beta$ -Ga <sub>2</sub> O <sub>3</sub> and their structural, optical and transport properties	J.-M. Chauveau	37
Artificial intelligence for on-the-fly analysis and control during oxide molecular beam epitaxy	Tiffany Kaspar	38
Structural and Optical Analyses of Ytterbium Implantation-Induced Effects and Defects in $\beta$ -Ga <sub>2</sub> O <sub>3</sub>	R. Ratajczak	39
Room-temperature cavity-polaritons in planar ZnO microcavities fabricated via a top-down process using bulk ZnO single crystals	K. Shima	40
Towards autonomous synthesis and characterization of oxide semiconductors and devices	Davi Febba	41
Thermochromic Property of Sandwiched VO <sub>2</sub> Thin Films in Dielectric Layers	Jazmyne Smith	42
VO <sub>2</sub> Phase Transition-Based Oscillators for Oscillatory Neural Networks	Zhaoyang (Frank) Fan	43
Epitaxial (Al <sub>x</sub> Ga <sub>1-x-y</sub> In <sub>y</sub> ) <sub>2</sub> O <sub>3</sub> alloys lattice matched to monoclinic Ga <sub>2</sub> O <sub>3</sub> substrates	Stephen Schaefer	44
Understanding and Controlling the Atomic Structure at NiO/Ga <sub>2</sub> O <sub>3</sub> PN Junction Interface	Chris Chae	45
Physics Informed Neural Network for Predicting Characteristics of $\beta$ -Ga <sub>2</sub> O <sub>3</sub> based FETs	Tasnia Jahan	46
Posters		49-63



**Monday**  
**03/03/2025**

# Advances in gallium oxide material and device technologies

Masataka Higashiwaki<sup>1,2</sup>

<sup>1</sup> Department of Physics and Electronics, Osaka Metropolitan University, Sakai, Osaka  
599-8531, Japan

<sup>2</sup> National Institute of Information and Communications Technology (NICT), Koganei,  
Tokyo 184-8795, Japan

Gallium oxide ( $\text{Ga}_2\text{O}_3$ ) had attracted little attention as a semiconductor for a long time. This situation has significantly changed in the past decade, and its research and development on materials and devices has become active mainly due to expectations for applications to next-generation power switching devices. Most of the distinguishing physical properties typified by the breakdown electric field are originated from the extremely large bandgap of 4.5 eV. Another important feature is the existence of large single-crystal bulks that can be synthesized by melt growth. Thanks to worldwide enthusiastic efforts, many important achievements on  $\text{Ga}_2\text{O}_3$  power field effect transistors (FETs), Schottky barrier diodes (SBDs), and  $p$ - $n$  heterostructure diodes have been reported until now [1].

In this talk, I will first provide a brief overview of milestone developments on  $\text{Ga}_2\text{O}_3$  devices at NICT since 2011. Then, current research and development on molecular beam epitaxy growth of nitrogen-doped  $\text{Ga}_2\text{O}_3$  thin films, and  $\text{Ga}_2\text{O}_3$  FETs and SBDs will be introduced.

## Acknowledgements

This work was supported by Ministry of Internal Affairs and Communications under a grant entitled “R&D of ICT Priority Technology (JPMI00316): Next-Generation Energy-Efficient Semiconductor Development and Demonstration Project” (second period) (in collaboration with Ministry of the Environment).

[1] M. Higashiwaki, IEEE Electron Devices Magazine **2**, 42 (2024).

## **CVD Diamond: Materials, Interfaces and Devices for Power, RF and Extreme Environments**

Robert J. Nemanich<sup>1</sup>, Franz A. Koeck<sup>1</sup>, Jesse Brown<sup>1</sup>, Aditya Deshmukh<sup>1</sup>, Mohamadali Malakoutian<sup>3</sup>, Gabriel Munro-Ludders<sup>1</sup>, Joshua Shoemaker<sup>1</sup>, Harshad Surdi<sup>1</sup>, Yu Yang<sup>1</sup>, Manpuneet Benipal<sup>2</sup>, Srabanti Chowdhury<sup>3</sup>, Stephen M. Goodnick<sup>1</sup>, David Smith<sup>1</sup>, Trevor J. Thorton<sup>1</sup>

[1] Arizona State University

[2] Advent Diamond Inc.

[3] Stanford University

Great strides in diamond wafer technology and diamond epitaxy have inspired new concepts for diamond electronics particularly for power conversion and RF applications. For diamond, the ultra wide bandgap supports high fields, the high electron and hole mobilities support low resistance and bipolar current transport, and the highest bulk thermal conductivity enables high power applications. At the center of this research is growth of high purity, epitaxial diamond layers by plasma enhanced CVD.

An alternative to substitutional impurity doping is interface charge transfer at a diamond-dielectric interface. Following the concept of modulation doping at heterostructure interfaces, ASU research has demonstrated a dielectric layer configuration that results in a nearly ten-fold mobility increase for the accumulated holes at the diamond interface.

High current PIN diodes prepared with epitaxial intrinsic and n-type (phosphorus doped) layers are described. The diodes operate much like a vacuum tube where injected carriers drift at the saturation velocity in the applied field. A specific example includes Schottky-PIN diodes that demonstrate current density greater than 100 kA/cm<sup>2</sup> and high frequency operation in receiver protect circuits. The same diodes show long term operation in high temperature and extreme environments

The impact of a new generation of diamond electronics will require the development of a Co-Design Ecosystem that will bring together scientists, engineers, manufacturing technologists, and societal leaders to enable the future electricity grid.

Research support: DOE Office of Science through the EFRC Program, National Science Foundation, ARPA-E, DARPA, and NASA.



## **Low-PBTS defect-engineered high-mobility metal-oxide BEOL-compatible transistors**

**Milan Pešić**

**Applied Materials Inc.**

As many times before, the scaling is facing a roadblock as current materials and device architectures are reaching its fundamental limits. In parallel to the material-device limitations, we are also on the brink of the architecture revolution as Von Neumann's architecture cannot follow the continuously increasing memory capacity and ever-rising workloads. Even though the path forward (comprised of in-memory-computing, monolithic integration, 3D stacking, and intelligent functional interconnects) is not fully clear, it will be enabled by functional energy-efficient materials and material-device engineering. Adoption of the new materials and devices can be accelerated and achieved only by understanding and diagnosing its properties and its evolution with lifetime. Only understanding of the materials and underlying physical mechanism can help us engineer novel superior devices of the future. Lead by this principle, we will investigate oxide-semiconductor materials and devices. We'll review what challenges they need to overcome to be integrated into logic and memory architectures. We will look in detail at the material phases, defects, vacancies, material changes, and underlying physical mechanisms governing mobility, variability, reliability, and others figures of merit of the devices they are integrated to. We will delve into the reliability features of the alternative channel materials, particularly 3D stacking-ready oxide semiconductors, and investigate the details of their density of states, mobility, and reliability. We will analyze physical mechanism and device reliability governed by channel defects, develop an ALD-grown IGZO channel material, and integrate it into a double-gated transistor test vehicle. Finally, interface-engineered IGZO-based transistors with high mobility and superior reliability (low PBTS) will be presented [1,2].

[1] B. Beltrando et al. "Low-PBTS defect-engineered high-mobility metal-oxide BEOL transistors" 2024 IEEE International Reliability Physics Symposium (IRPS).

[2] S. Nahar et al. "A Study on High Performance, Dual-Gate a-IZO/a-IGZTO TFTs with Excellent Stability" IEEE Electron Device Letters 2024

# Advances in Ga<sub>2</sub>O<sub>3</sub> Power Device Development

Kohei Sasaki and Akito Kuramata

Novel Crystal Technology, Inc.

2-3-1 Hirosedai, Sayama, Saitama, 350-1328, Japan

sasaki@novelcrystal.co.jp

$\beta$ -Ga<sub>2</sub>O<sub>3</sub> is the candidate material for high-power device applications.<sup>1)</sup> In the last decade, 4-inch single-crystal substrates were demonstrated by using the edge-defined film-fed growth method, and high-quality homoepitaxial films were also developed by using the halide vapor phase epitaxy (HVPE) method. A few years ago, large 100-A class Schottky barrier diodes (SBDs) were fabricated on HVPE grown films with a killer defect density of about 1 /cm<sup>2</sup> (Fig.1). To realize the full potential of Ga<sub>2</sub>O<sub>3</sub>, a trench MOS structure was incorporated in the SBD structure. That SBD, called a MOSSBD, showed a smaller on-resistance than that of SiC SBDs. Ga<sub>2</sub>O<sub>3</sub> junction barrier Schottky diodes were developed by using a p-NiO/n-Ga<sub>2</sub>O<sub>3</sub> hetero pn junction. This concept may be a solution to the problem of a lack of p-type Ga<sub>2</sub>O<sub>3</sub>. Currently, a demonstration of the high blocking voltage is proceeding. A 5-kV FinFET was demonstrated by using a thick HVPE-grown drift layer with a low donor concentration. However, the FinFET structure has a rather low gate threshold voltage. Therefore, we developed inversion-type MOSFET by using a nitrogen-doped well region. The device showed a high enough threshold voltage of about 6 V and a high breakdown voltage of over 1 kV. In the near future, we will demonstrate large-current, high-blocking-voltage Ga<sub>2</sub>O<sub>3</sub> MOSFETs.

1) K. Sasaki, Appl. Phys. Express. **17**, 090101 (2024).

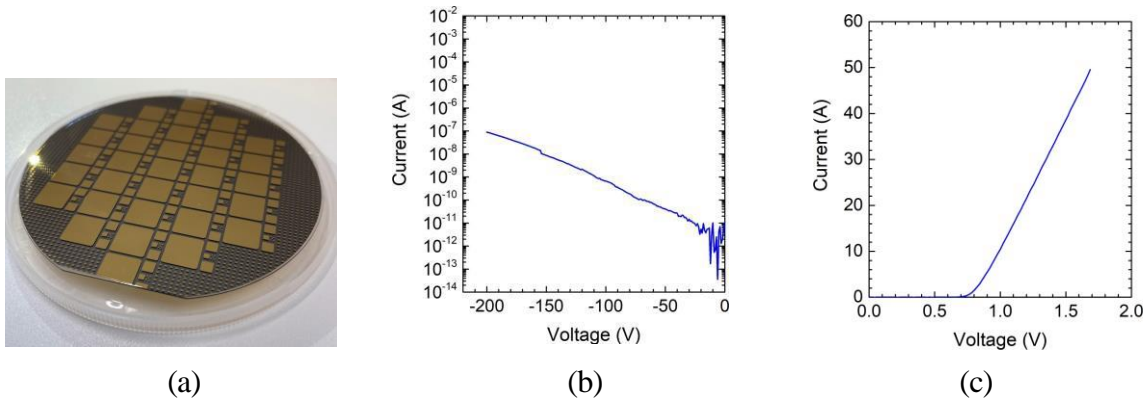


Fig.1. (a) Photograph, (b) reverse, and (c) forward characteristics of 10 mm square SBDs on a 100-mm  $\beta$ -Ga<sub>2</sub>O<sub>3</sub> epi wafer.

# **Unconventional doping methods for Ga<sub>2</sub>O<sub>3</sub> and ZnO**

Farida Selim

Arizona State University

Abstract to be added.

# Origins and dynamic properties of midgap recombination centers in ZnO

**S. F. Chichibu<sup>1\*</sup>, A. Uedono<sup>2</sup>, S. Ishibashi<sup>3</sup>, and K. Shima<sup>1</sup>**

<sup>1</sup>IMRAM-Tohoku Univ., 2-2-1 Katahira, Aoba-ku, Sendai, Miyagi 980-8577, Japan

<sup>2</sup>Division of Appl. Phys., Univ. of Tsukuba, Tsukuba, Ibaraki 305-8573, Japan

<sup>3</sup>CD-FMat, AIST, Tsukuba, Ibaraki 305-8568, Japan

\*presenting author, e-mail: [chichibulab@yahoo.co.jp](mailto:chichibulab@yahoo.co.jp)

Wurtzite (w) ZnO and wurtzite / rocksalt (rs)  $\text{Mg}_x\text{Zn}_{1-x}\text{O}$  alloys are an excellent candidate for the use in NUV to FUV light-emitting diodes (LEDs) [1] and radiation-resistant transistors. For improving LED performances, accurate understanding of the origins and dynamic properties of deleterious midgap recombination centers (MGRCs) is essential, where MGRCs include nonradiative recombination centers (NRCs) and deep-state radiative recombination centers (DRRCs), both obey the Shockley-Read-Hall statistics.

As quite low dislocation density bulk ZnO substrates grown by the hydrothermal technique [2] have been commercially available, the importance of point defects such as Zn vacancies ( $V_{\text{Zn}}$ ) [3] on the nonradiative recombination process [4] has been recognized from the initial stage of the ZnO LED research [1]. For example, the authors have studied various quality ZnO bulk crystals [2,5] and epilayers [1,3,4] by the complementary use of time-resolved photoluminescence (TRPL) [4] and positron ( $e^+$ ) annihilation spectroscopy (PAS) [3] measurements to identify vacancy complexes comprising  $V_{\text{Zn}}$  and O vacancies ( $V_{\text{O}}$ ), namely  $V_{\text{Zn}}V_{\text{O}}$  "divacancies" as the origin of the major intrinsic NRCs in n-type ZnO, because the nonradiative lifetime ( $\tau_{\text{NR}}$ ) for the near-band-edge (NBE) emission decreased with increasing the concentration of  $V_{\text{Zn}}V_{\text{O}}$  [6].

In this presentation, accurate atomic structure of the intrinsic and extrinsic MGRCs in n-ZnO and their hole capture-cross-section ( $\sigma_p$ ) will be discussed by presenting the results of TRPL and PAS measurements on ZnO epilayers grown under different conditions [1,3,4] and bulk crystals [2] either irradiated by a high energy (8 MeV) proton beam [5] or polished or etched by various methods.

As shown in Fig. 1, room-temperature photoluminescence lifetime ( $\tau_{\text{PL}}$ ) for the NBE emission of unintentionally-doped ZnO decreased with increasing  $V_{\text{Zn}}V_{\text{O}}$  concentration,  $[V_{\text{Zn}}V_{\text{O}}]$ , while  $\tau_{\text{PL}}$  of transition-metal (TM)-doped samples were dominated by the TM concentration. MGRC concentration ( $N_{\text{MGRC}}$ ) lower than  $10^{15} \text{ cm}^{-3}$  should be maintained to observe intrinsic optical properties of semiconductor ZnO.

We thank Professors M. Kawasaki, A. Ohtomo, A. Tsukazaki, K. Koike, M. Yano, and S. Gonda for providing the samples and Dr. K. Furusawa, Dr. K. Hazu, and K. Kikuchi for the help with experiments. This work was supported in part by Crossover Alliance under MEXT, Japan.

[1] A. Tsukazaki *et al.*, *Nature Mater.* **4**, 42 (2005). [2] E. Oshima *et al.*, *J. Cryst. Growth* **260**, 166 (2004). [3] A. Uedono *et al.*, *J. Appl. Phys.* **93**, 2481 (2003). [4] S. F. Chichibu *et al.*, *Semicond. Sci. Technol.* **20**, S67 (2005); *J. Appl. Phys.* **99**, 093505 (2006). [5] K. Koike *et al.*, *J. Appl. Phys.* **123**, 161562 (2018). [6] S. F. Chichibu *et al.*, *J. Appl. Phys.* **127**, 215704 (2020).

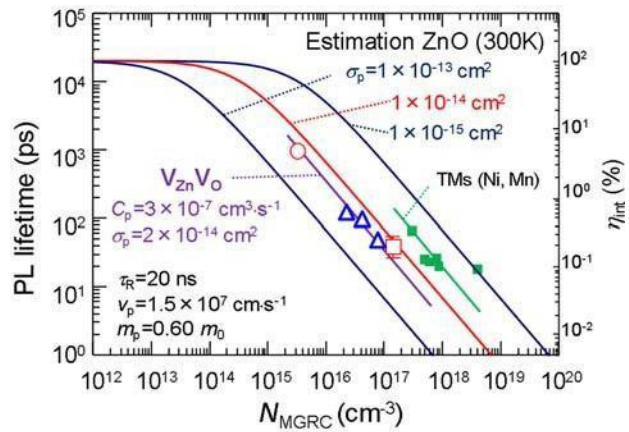


Fig. 1. PL lifetime ( $\tau_{\text{PL}}$ ) and corresponding internal quantum efficiency ( $\eta_{\text{int}}$ ) for the NBE emission of n-ZnO at 300 K as a function of MGRC concentration ( $N_{\text{MGRC}}$ ) [6].

# **Towards In Situ Visualization of Nanoscale and Atomic-Level Dynamics and Transport in Oxides**

**Peter Crozier**

**Arizona State University**

The ability to design structures that can regulate and control the transport functionalities of electroceramics for applications in a wide range of devices requires a fundamental understanding of structural dynamics and migration. Elucidating the relationship between local structure and transport remains an ongoing challenge for both experimental and computational techniques. Modern transmission electron microscopy (TEM) allows the structure and composition of electroceramics to be characterized down to the atomic level. However, a goal of *in situ* electron microscopy is to characterize the transport variations and pathways with high spatial resolution. Can transport/diffusion processes be directly observed at the atomic level? Here we use aberration corrected *in situ* transmission electron microscopy and deep learning denoising techniques to explore oxygen ionic dynamics and diffusion in cerium dioxide. With *in situ* light illumination and electron holography, we also investigate variations in the induced electric fields at nanoparticle surfaces that can drive transport processes. We demonstrate local sensing of photo-induced electronic conductivity in nanoscale particles of strontium titanate. This presentation will discuss what is currently possible from *in situ* TEM approaches and how the field is likely to evolve over the near future.

## **Acknowledgements**

We gratefully acknowledge the support of the following NSF grants to ASU (OAC 1940263, 2104105 and DMR 184084 and 1920335). The authors acknowledge HPC resources available through ASU, and NYU as well as the High Resolution Electron Microscopy Eyring Materials Center at Arizona State University.

# {ZnCdO/ZnMgO} SLs *in situ* Eu-doped growth by PA-MBE

E. Przeździecka<sup>1</sup>, A. Lysak<sup>1</sup>, A. Wierzbicka<sup>1</sup>, S. Magalhaes<sup>2</sup>,  
P. Dłużewski<sup>1</sup>, M. Szot<sup>3</sup>, R. Jakiela<sup>1</sup>, Y. Zhydashvsky<sup>1</sup>, Z. Khosravizadeh<sup>1</sup>, A. Kozanecki<sup>1</sup>

<sup>1</sup> Institute of Physics, Polish Academy of Sciences, 02-668, Warsaw, Poland

<sup>2</sup> Instituto de Plasmas e Fusão Nuclear, Instituto Superior Técnico, Universidade de Lisboa, 1049-001, Lisboa, Portugal

<sup>3</sup> International Research Centre MagTop, Institute of Physics, Polish Academy of Sciences, Aleja Lotników 32/46, 02-668 Warsaw, Poland.

Wide-band gap semiconductors doped with rare earth elements (RE) have attracted considerable attention due to their unique properties and potential applications across a wide range of fields. For instance, doping ZnO-based structures with RE presents a promising approach for realizing LEDs operating in the visible spectrum. Among rare-earth elements, Europium (Eu) exhibits unique luminescence properties, particularly red emission around 615 nm, attributed to the intra-4f-shell transition. However, the efficiency of Eu luminescence strongly depends on the host matrix. One of the promising host materials for Eu doping is ZnO. The bandgap energy of II-VI oxides can be further modulated from the visible to the deep UV region by forming ternary alloys e.g.: ZnCdO, ZnMgO, and CdMgO. While most studies focus on the investigation of Eu-doped ZnO the properties of oxide-based quantum structures doped with Eu ions remain relatively unexplored. To achieve higher output power, the excitation efficiency of the Eu ions must be enhanced, for instance, by increasing the carrier density around Eu ions. This can be accomplished by doping Eu into quantum well (QW) layers positioned between barrier layers. In such structures, the carrier density increases as carriers are confined within the Eu-containing quantum wells, facilitating more efficient energy transfer to Eu ions. Consequently, investigating oxide-based quantum structures doped with Eu could offer greater potential for future optoelectronic applications.

PA-MBE is considered the most suitable technology for depositing quantum structures due to its precise control of sublayer thickness and composition, as well as allowing the accurate *in situ* incorporation of RE ions within the structure without damaging the crystal lattice<sup>[1]</sup>. Also, this method can solve the problem of phase separation due to the different crystal structures of CdO, MgO and ZnO<sup>[2,3]</sup>. This investigation focuses on *in situ* Eu-doped ZnCdO/ZnMgO and ZnCdO/ZnO superlattices (SLs) of varying sublayer thicknesses, grown on Al<sub>2</sub>O<sub>3</sub>. We studied the structural and optical properties of the Eu-doped ZnCdO/ZnMgO and ZnCdO/ZnO SLs through TEM, X-ray diffraction, UV-Vis spectroscopy, secondary-ion mass spectrometry (SIMS), and cathode- and photo- luminescence (CL and PL) assessments. TEM, XRD, and SIMS measurements confirmed high quality of periodic structures. The analysis of TEM and XRD within the framework of dynamical theory allowed us to determine the sublayers thicknesses. We carried out CL measurements both at room and low temperatures of Eu-doped superlattice structures. From this study it was found that adding Mg to ZnO barriers and reducing the ZnCdO:Eu QW thickness enhanced the red emission related to Eu<sup>3+</sup> ions<sup>[4]</sup>. Furthermore, post-annealing treatments at 700°C in an oxygen environment notably increased red emission intensity, although with a further increase in temperature its thermal quenching was observed. Temperature-dependent CL and PL measurements demonstrated the stable of Eu<sup>3+</sup> emission in the temperature up to 300 K. These findings underscore the promising potential of *in situ* Eu-doped ZnCdO/ZnMgO and ZnCdO/ZnO SLs for advanced optoelectronic device applications.

This work was supported in part by the Polish National Science Center, Grants 2021/41/B/ST5/ 00216

[1] J. A. Mathew, et al., J. Lumin. 251 (2022), 119167.

[2] A. Lysak, et al. Cryst. Growth Des. 23 (2023), 134.

[3] E. Przeździecka, et al. Nanoscale Res. Lett. 16 (2021), 1.; E. Przeździecka et al. *Crystal Growth & Design* 2022 22 (2), 1110-1115

[4] A. Kozanecki, et al., Appl. Phys. Lett. 119 (2021), 112101.

## Ion irradiation induced phase transformation in $\beta$ -Ga<sub>2</sub>O<sub>3</sub> through in-situ ion irradiation in a TEM

Djamel Kaoumi<sup>a</sup>, Bruno Caruso<sup>a</sup>, Angelica Lopez Morales<sup>a</sup>, Ryan Schoell<sup>b</sup>, Andrej Kuznetsov<sup>c</sup>, Farida A Selim<sup>d</sup>

<sup>a</sup>North Carolina State University, Department of Nuclear Engineering, Raleigh, NC

<sup>b</sup>Sandia National Laboratories

<sup>c</sup>University of Oslo, Oslo, Norway

<sup>d</sup>Arizona State University, AZ, United States

This research is part of a project which explores the use of Ga<sub>2</sub>O<sub>3</sub> as a semiconductor in detectors. Particularly this work aims to examine the effects of radiation damage and temperature on the stability and semiconductor properties of gallium oxide. Along with considering how the semiconductor properties (electrical and optical) are affected, it is important to understand the irradiation response of a Ga<sub>2</sub>O<sub>3</sub> single crystal in terms of its structure using in-situ irradiation in a TEM. Characterizing the phases present at different irradiation doses through the use of electron diffraction can reveal transition doses and, in turn, phase stability. This is all the more important than Ga<sub>2</sub>O<sub>3</sub> is known to be polymorphic that can be present in six different phases:  $\alpha$ ,  $\beta$ ,  $\gamma$ ,  $\delta$ ,  $\varepsilon$  and  $\kappa$ . Monitoring radiation effects in terms of possible phase changes and radiation damage (black dot and loop formation) is critical to understanding the possible changes in physical properties. In the literature, a phase transformation from  $\beta$  to  $\kappa$  was reported in bulk Ga<sub>2</sub>O<sub>3</sub> at room temperature for a given dose [1]. Later, it was reported that the actual phase forming was  $\gamma$  and not  $\kappa$ . In order to bring more light onto this irradiation induced phase transformation, a systematic study is needed not only to further investigate the mechanisms of the phase transformation in Ga<sub>2</sub>O<sub>3</sub> but also the effect of temperature in a timely manner (which has not been reported in the literature). For that matter, in situ irradiations in a TEM were done using 1 MeV Kr ion irradiation of Ga<sub>2</sub>O<sub>3</sub> TEM foils processed through Focused Ion Beam Lift out method. The gallium oxides samples were grown either by Czochralski (CZ) or Edge-defined Film-Fed Growth (FFG) techniques. Detailed Diffraction Pattern analysis was performed as a function of irradiation dose, which brought more insight onto the phase transformation and temperature dependence, which will be reported in this presentation. The experiments showed that phase transformation does not require implantation of ions as the ions travel through the foil in our case. The possible mechanism will be discussed in this presentation.

This work was supported as part of Nuclear Science and Security Consortium (NSSC) (DE-NA0003996) and experiments at the IVEM, an NSUF facility, were made possible thanks to DOE through the NSUF award 20-19163.

**Tuesday**  
**03/04/2025**



# **Growth and basic physical properties of bulk single crystals of transparent semiconducting oxides**

**Zbigniew Galazka**

Leibniz-Institut für Kristallzucht (IKZ), Max-Born-Str. 2, 12489 Berlin, Germany

E-mail: zbigniew.galazka@ikz-berlin.de

Transparent semiconducting oxides (TSOs) constitute a class of oxide materials combining both semiconducting behaviour and transparency in the visible / UV spectral region arising from wide- or ultrawide bandgaps. The TSOs drive an extensive research towards novel devices and applications in electronics, opto-electronics, photovoltaics, radiation detection, and gas sensing among others.

In most cases, a device development depends on the availability of bulk single crystals, mainly functioning as lattice-matched substrates for homoepitaxial growth and power device fabrication in both lateral and vertical architectures. High melting points and thermal instability of the TSOs make the crystal growth directly from the melt difficult and challenging, often requiring novel approaches in crystal growth technology. All the TSO compounds to be discussed were grown at IKZ and include binary ( $\beta$ -Ga<sub>2</sub>O<sub>3</sub>, In<sub>2</sub>O<sub>3</sub>, SnO<sub>2</sub>, r-GeO<sub>2</sub>, ZnO), ternary ( $\beta$ -(Al<sub>x</sub>Ga<sub>1-x</sub>)<sub>2</sub>O<sub>3</sub>, BaSnO<sub>3</sub>, ZnSnO<sub>3</sub>, MgGa<sub>2</sub>O<sub>4</sub>, ZnGa<sub>2</sub>O<sub>4</sub>), and quaternary (Zn<sub>1-x</sub>Mg<sub>x</sub>Ga<sub>2</sub>O<sub>4</sub>, InGaZnO<sub>4</sub>) systems [1 - 4].

An overview will include main aspects of crystal growth, doping with various elements, annealing, and basic physical properties of obtained crystals. A particular attention will be paid to electrical properties of bulk TSO single crystals, which attract attention in both academia and industry, mainly for high-power electronic devices to improve voltage conversion efficiency.

This work was funded by the Deutsche Forschungsgemeinschaft (DFG) project nos. FO558/3-1, GA2057/2-1, and GA2057/5-1; Bundesministerium für Bildung und Forschung (BMBF) project nos. 03VP03712 and 16ES1084K; and Leibniz-Gemeinschaft Senatsausschuss Wettbewerb (SAW) project nos. K74/2017 and K417/2021.

[1] Z. Galazka; “Transparent Semiconducting Oxides – Bulk Crystal Growth and Fundamental Properties”, Jenny Stanford Publishing (2020).

[2] Z. Galazka; “Growth of bulk  $\beta$ -Ga<sub>2</sub>O<sub>3</sub> single crystals” in “Comprehensive Semiconductor Science and Technology 2nd Ed.”, Ed. R. Fornari, Elsevier (2025)

[3] Z. Galazka, K. Irmischer, M. Pietsch, S. Ganschow, D. Schulz, D. Klimm, I. M. Hanke, T. Schroeder, M. Bickermann; J. Mater. Res. 36 (2021) 4746-4755.

[4] Z. Galazka, R. Blukis, A. Fiedler, S. Bin Anooz, J. Zhang, M. Albrecht, T. Remmele, T. Schulz, D. Klimm, M. Pietsch, A. Kwasniewski, A. Dittmar, S. Ganschow, U. Juda, K. Stolze, M. Suendermann, T. Schroeder, M. Bickermann; Phys. Status Solidi B (2024) 2400326.

# On the relationship between atomic and electronic structure on Ln-bearing oxides

Blas Pedro Uberuaga<sup>1</sup>, Vancho Kocovski<sup>1</sup>, Anjana A. Talapatra<sup>1</sup>, Benjamin K. Derby<sup>2</sup>, and Ellis R. Kennedy<sup>2</sup>

<sup>1</sup>Materials Science and Technology Division, Los Alamos National Laboratory, Los Alamos, NM, USA

<sup>2</sup>Materials Physics and Applications Division, Los Alamos National Laboratory, Los Alamos, NM, USA

Metastable states of matter are of great interest as they offer the promise of novel functionality. They are also a natural consequence of radiation induced changes in the structure of irradiated solids. In oxides, radiation can induce chemical disorder and even amorphization. While significant attention has been given to the impact those changes have on the atomic properties of the material, the corresponding changes in the electronic structure have received less. Here, using density functional theory, we consider how the electronic structure varies with potential metastable structures in two classes of lanthanide bearing oxides - pyrochlores and inter-lanthanide sesquioxides. We find that the changes depend strongly on both the crystal structure and crystal chemistry of the compound, with for example disordering and amorphization either increasing or decreasing the band gap depending on the chemistry. Our calculations are validated by electron energy loss spectroscopy measurements for two pyrochlore compounds in which amorphization does reduce the band gap, consistent with our calculations on these two compounds. Our results highlight the relationship between atomic and electronic structure and how radiation can be used to modify and potentially control the electronic properties of oxides.

## Defect modeling and damage buildup in ion-bombarded oxides

Przemysław Jóźwik<sup>1</sup>, Renata Ratajczak<sup>1</sup>, Cyprian Mieszczyński<sup>1</sup>, Joanna Matulewicz<sup>1</sup>,  
Jacek Jagielski<sup>1</sup>, Andrzej Turos<sup>1</sup>, and Frederico Garrido<sup>2</sup>

<sup>1</sup> National Centre for Nuclear Research, Otwock, Poland

<sup>2</sup> IJCLab, Université Paris-Saclay-CNRS, 91405 Orsay Campus, France

Radiation effects upon ion bombardment in oxide semiconductors have been studied extensively over the past decades. Ion channeling is mainly used in such research as it is sensitive to a disorder present in the crystalline materials. However, the light ions used in this technique interact differently with different types of defects, being either directly backscattered or dechanneled from the channeled trajectories. Analytical models can hardly distinguish between point and extended defects, so relative damage is usually used instead. An important step forward has been the recent development of the Monte Carlo *McChasy* simulation code<sup>1</sup>, which allows the distinction between randomly displaced atoms and edge dislocations or dislocation loops. It has been shown that the growth of extended defects upon ion bombardment and their role in structural transformations at specific fluences of the bombarding ion beam are by no means negligible in oxides. In addition, complementary techniques such as high-resolution X-ray diffraction (HRXRD) and high-resolution transmission electron microscopy (HRTEM) have provided important data that are essential for elucidating the mechanism of damage accumulation, which also depends on the ion species.

The multi-step damage accumulation process will be shown and compared for selected oxides such as SrTiO<sub>3</sub>, ZrO<sub>2</sub>, MgAl<sub>2</sub>O<sub>4</sub> (spinel), ZnO, and Ga<sub>2</sub>O<sub>3</sub>. Experimental data will be reviewed and defect transformation models will be discussed. HRTEM will be presented as a source of geometric parameters of dislocations along with the modeling of defects provided by molecular dynamics. HRXRD will be reported to show the strain build-up upon ion bombardment in the implanted region, leading to plastic deformation due to dislocation slip once the critical stress value is reached. The transition to the amorphous state can eventually occur at high impurity concentration and is apparently due to the defect-impurity interaction. This leads to the conclusion that microstructural transformations driven by lattice strain leading to multistep damage accumulation is a typical phenomenon in ion bombarded oxides. Some implications of this model for practical applications will also be presented.

---

<sup>1</sup> <https://www.ncbj.gov.pl/en/mcchasy>

## Acceptor complexes in ZnO – effect of strain, surface proximity and carbon content

Elżbieta Guziewicz and Oksana Volnianska

*Institute of Physics, Polish Academy of Sciences, Al. Lotnikow 32/46, 02 668 Warsaw, Poland*

As recently established in experimental and theoretical works, defect complexes including native point defects, hydrogen and possibly a dopant determine electrical conductivity of ZnO in a wide range as they introduce shallow and deep donor and acceptor states in the bandgap. This knowledge seems discouraging because the control of conductivity, and in particular the achievement of acceptor conductivity, requires the simultaneous tuning of point defects and dopants, which is difficult to achieve. Our investigations indicate, however, that this goal seems to be achievable, provided that the process of growth ZnO of layers is consciously carried out.

In the presentation we will show the experimental cathodoluminescence (CL) and scanning photoelectron microscopy (SPEM) measurements performed on ZnO:N layers that allow sampling of a single microcrystallite in the films cross-section [1-3]. The results account for grouping acceptor and donors in separate domains/crystallites. This phenomenon is found to be very common provided the ZnO films are grown under O-rich conditions and nitrogen is introduced in the form of the –NH chemical group. Density Functional Theory calculations point out that the complexes involving zinc vacancy ( $V_{Zn}$ ), hydrogen and nitrogen provide complexes-related acceptor states [4]. Hydrogen stabilizes formation of the  $V_{Zn}N_O$  complex, but the appearing  $V_{Zn}N_OH$  complex is found to be a deep acceptor. DFT calculations show that compressive strain and/or surface proximity facilitate the formation of acceptor complexes, so they are easily created under appropriate strain/microstrain conditions or near the surface. This theoretical finding may explain the origin of acceptor and donor grouping in different crystallites. A closer insight into the electronic structure of a single crystallite performed by SPEM experiment reveals that carbon present in a form of –CH group facilitates the formation of acceptor states, as seen by the modification of the valence band shape. According to DFT calculations,  $C_iH_x$  group is stable in the ZnO crystal lattice and creates C-H-O bond states. The calculated migration properties show that complexes such as  $V_{Zn}(NH)_O$  are easily formed in the presence of the interstitial  $C_iH_2$  group as it leads to lowering of the migration energy of  $V_{Zn}$  by 0.8 eV and to 0 eV in the ZnO and ZnO:N, respectively [5].

**Acknowledgements** The study was supported by the Polish NCN Project DEC-2018/07/B/ST3/03576

- [1] E. Guziewicz, O. Volnianska et al., **Phys. Rev. Appl.** **18** 044021 (1-13) (2022)
- [2] E. Guziewicz, E. Przedziecka et al., **ACS Appl. Mat. Interfaces** **9**, 26143-26150 (2017)
- [3] S. Mishra, B.S. Witkowski et al., **Phys. Stat. Sol. A** **2022**, 2200466 (1-11)
- [4] O. Volnianska, V.Yu. Ivanov, L. Wachnicki, E. Guziewicz, **ACS Omega** **2023**, *8*, 43099
- [5] E. Guziewicz, S. Mishra, M. Amati, L. Gregoratti and O. Volnianska, **Nanomaterials** **2025**, *15*, 30

## Persistent optical phenomena in oxide semiconductors

M.D. McCluskey,<sup>1-2</sup> M.M. Santillan,<sup>1</sup> and J.S. McCloy<sup>2</sup>

<sup>1</sup>*Department of Physics and Astronomy, Washington State University, Pullman, Washington 99164-2814, USA*

<sup>2</sup>*Institute of Materials Research, Washington State University, Pullman, Washington, USA 99164-2711*

The interaction of transparent oxide semiconductors with light is a central issue for a range of applications. Persistent effects could be exploited for holographic memory or optically defined circuits. They may also be detrimental to device operation. Large, room-temperature persistent photoconductivity (PPC) has been observed in potassium tantalate (KTaO<sub>3</sub>, KTO) after annealing in a hydrogen atmosphere. The conductivity increases by four orders of magnitude after exposure to UV light, which persists for years after the light is turned off. Photochromism, due to a defect absorption peak in the visible region of the spectrum, also occurs. In Cu-doped gallium oxide ( $\beta$ -Ga<sub>2</sub>O<sub>3</sub>), photochromism was observed after exposure to sub-bandgap light.

Hydrogen is believed to play a key role in these persistent phenomena. In our proposed model, a photon excites substitutional hydrogen (a proton inside an oxygen vacancy), making the defect unstable. The proton leaves and binds to a host oxygen atom, forming an O-H bond that is observed with IR spectroscopy. An oxygen vacancy is left behind. Because oxygen vacancies in KTO are shallow donors, this process results in PPC. In  $\beta$ -Ga<sub>2</sub>O<sub>3</sub>:Cu, however, the oxygen vacancy neighbors a Cu acceptor. In that case, photoexcitation results in the rare Cu<sup>3+</sup> state, which absorbs visible light. The effect can be “erased” by annealing at 300-400°C.

## **Positron Annihilation Spectroscopy (PAS) of PbO direct-photoconductor material deposited at low temperature for the development of TFT-based x-ray imaging.**

J.M. Gaudet<sup>1,2,\*</sup>, T. Wu<sup>2</sup>, A. Stieh<sup>3</sup>, J. Rado<sup>3</sup>, A. Reznik<sup>3</sup>, A.P. Knights<sup>2</sup> and P. Mascher<sup>2</sup>

<sup>1</sup>*Department of Nuclear Operations and Facilities, McMaster University, Hamilton, Canada*

<sup>2</sup>*Department of Engineering Physics, McMaster University, Hamilton, Canada*

<sup>3</sup>*Department of Physics, Lakehead University, Thunder Bay, Canada*

\*email: [gaudej4@mcmaster.ca](mailto:gaudej4@mcmaster.ca)

Direct photoconductors, which convert x-rays directly to charge carriers, deposited on a thin-film transistor array, can be used to produce x-ray images with better spatial resolution than similar devices made with indirect photoconductors (which involves the production of visible light as an intermediate step.) Direct photoconductive x-ray imagers have been commercialized using stabilized amorphous Se, and are optimized for mammography using 20keV x-rays. Applications using, e.g., 60keV x-rays for chest imaging are not yet feasible due to the relatively low atomic number of Se and the inability to produce sufficiently thick stabilized a-Se films [1]. The discovery of dense, amorphous PbO that can be deposited at low temperature (<200C) offers the possibility of a 60keV photoconductive x-ray imager [2], but two immediate practical problems inhibit this possibility: 1) a-PbO films are prone to cracking with increasing thickness, with the onset of this behaviour occurring at thicknesses of less than ten microns, and 2) the charge collection efficiency of films produced so far is very low, likely due to charge traps associated with vacancy-type defects.

Variable-energy, Doppler-broadened PAS yields information about vacancy-type defects within a thin-film sample. The variable energy of the positron beam allows implantation of positrons into different depths of the film. Upon thermalization, positrons are repulsed from positive ion cores and become trapped in vacancy-type defects (or in other open volumes in the material.) The positrons eventually annihilate with electrons in the vicinity of the trapping site, and the resulting annihilation photons are Doppler shifted by an amount determined by the energy of the electron. By measuring the energy spectrum of the annihilation radiation, the proportion of positrons annihilating with core and valence electrons can be roughly calculated. Thus, the defect structure of a set of otherwise similar samples can be compared and, ideally, correlated to some other known systematic variation between them (i.e. synthesis conditions.) This talk will present such a study on a set of amorphous PbO samples.

[1] S. Kasap, J. B. Frey, G. Belev, O. Tousignant, H. Mani, J. Greenspan, L. Laperriere, O. Bubon, A. Reznik, et al, *Sensors*, 2011, 11, 5112 —5157

[2] O. Semeniuk, A. Csik, S. Kökényesi and A. Reznik, *J. Mater. Sci.*, DOI: 10.1007 / s10853-017-0998-5

# Photoluminescence of spinel $\text{MgGa}_2\text{O}_4$ and $\text{ZnGa}_2\text{O}_4$ thin films grown by molecular beam epitaxy

Jianlin Liu\*, Tianchen Yang, Chengyun Shou, Abdullah Almuhtabi, Edward Zhu, and Quazi Sanjid Mahmud

*Department of Electrical and Computer Engineering, University of California, Riverside, CA 92521, USA*

*\* Correspondence should be addressed to Jianlin Liu (email: [jianlin@ece.ucr.edu](mailto:jianlin@ece.ucr.edu), Tel: 1-9518277131, Fax: 1-9518272425)*

## ABSTRACT:

This study explores photoluminescence (PL) characteristics of spinel  $\text{MgGaO}$  and  $\text{ZnGaO}$  semiconductor thin films grown via plasma-assisted molecular beam epitaxy. By varying Mg atomic percentages ranging from 0 to 15%, we reveal distinct phase boundaries:  $\text{MgGaO}$  films exhibit pure  $\beta$ -phase at lower Mg concentrations (0-4%), a coexistence of  $\beta$ -phase and spinel phase at intermediate Mg levels (7-12%), and complete transition to pure spinel phase at higher Mg concentrations (13-15%). Structural analysis via X-ray diffraction confirms these transitions and identifies corresponding changes in lattice parameters. Comprehensive PL studies, encompassing room temperature measurements as well as power and temperature-dependent analyses, have revealed distinct emission spectra and mechanisms intrinsic to  $\beta$ - $\text{MgGaO}$  and spinel  $\text{MgGa}_2\text{O}_4$ . These investigations have elucidated defect energy levels associated with various entities such as self-trapped holes (STH), deep donors from oxygen vacancies, deep acceptors involving Mg on Ga sites, and acceptor complexes formed with Ga and O. Similar properties were observed from  $\text{ZnGaO}$  thin films. This research enhances our understanding of  $\text{MgGaO}$  and  $\text{ZnGaO}$  alloy phase evolution and provides insights for advancing optoelectronic applications of these spinel  $\text{MgGa}_2\text{O}_4$  and  $\text{ZnGa}_2\text{O}_4$  materials.

# Internal and External Control of Excitons in Colloidal Quantum Dots

**J. A. Hollingsworth**

*Center for Integrated Nanotechnologies & Microelectronics Science Research Center (MSRC): Co-design and Heterogeneous Integration in Microelectronics for Extreme Environments (CHIME): Materials Physics & Applications Division, Los Alamos National Laboratory, Los Alamos, New Mexico, USA*

Colloidal quantum dots (cQDs) synthesized in simple laboratory flasks are finding real-world applications in demanding technologies from displays and lighting to photovoltaics and photodetectors. In the future, cQDs may be the basis for single-photon devices in quantum networks. Beyond quantum-size control, we pursue an expanded “structural toolbox” to synthetically engineer new quantum emitters with targeted photophysical properties, including non-blinking behavior, biexciton enhancement, dual-color emission.<sup>1-9</sup> Taking advantage of their solution-phase processibility, we prepare cavity- or antenna-coupled cQD hybrid materials using, e.g., deterministic, direct-write nanointegration.<sup>10,11</sup> The former—precision synthesis—affords *internal control* over excitonic properties,<sup>1-9</sup> while the latter—hybrid materials fabrication—affords *external control* via local environmental effects.<sup>10-14</sup>

## References

- [1] Singh, A. et al. *Small Sci.* **3**, 2300092 (2023).
- [2] Krishnamurthy, S. et al. *ACS Nano* **15**, 575 (2021).
- [3] Dennis, A. M. et al. *Adv. Funct. Mater.* **29**, 1809111-1-10 (2019).
- [4] Hanson, C. J. et al. *J. Am. Chem. Soc.* **139**, 11081 (2017).
- [5] Mishra, N. et al. *Nature Commun.* **8**, 15083-1-9 (2017).
- [6] Mangum, B. D., et al. *Nanoscale* **6**, 3712 (2014).
- [7] Dennis, A. M. et al. *Nano Lett.* **12**, 5545 (2012).
- [8] Ghosh, Y. et al. *J. Am. Chem. Soc.* **134**, 9634 (2012).
- [9] Chen, Y. et al. *J. Am. Chem. Soc.* **130**, 5026, (2008).
- [10] Lubotzky, B. et al. *Nano Lett.* **24**, 640 (2024).
- [11] Abudayyeh, H. et al. *APL Photonics* **6**, 036109-1-7 (2021).
- [12] Mishra, S. et al. *ACS Nano* **18**, 8663 (2024)
- [13] Dolgoplova et al. *Nanoscale Horiz.* **7**, 267 (2022).
- [14] Gao, Y. et al. *Adv. Optical Mater.* **3**, 39 (2015).

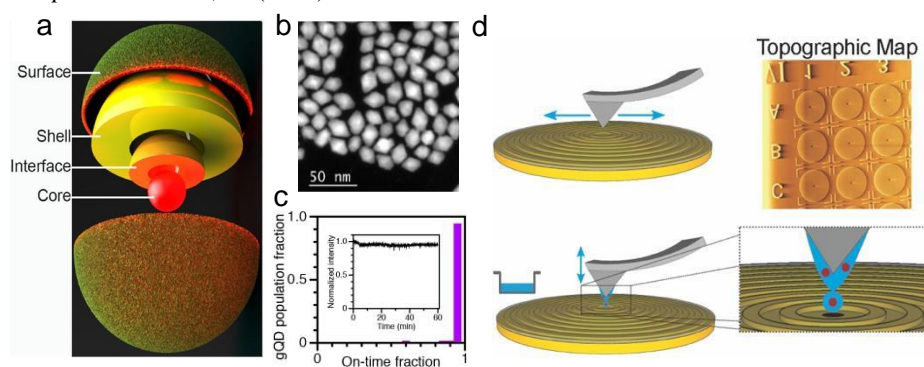


**Figure.** (a) Schematic illustration of the components of a core/shell QD accessible for precision synthetic manipulation and *internal* exciton control. (b),(c) CdSe/CdS core/thick-shell “giant” QDs (gQDs): electron microscopy images (b) and plot of population fraction versus on-time fraction revealing extreme non-blinking/non-photobleaching photoluminescence (c);<sup>1</sup> such *on-demand photon emission now demonstrated for gQDs from blue-green to the full telecommunications window*.<sup>1-9</sup> (d) “Direct-write” method for coupling quantum emitters to nanoantennas and photonic structures for *external* exciton control:<sup>10-11</sup> (top) AFM scan of area of interest; right panel shows image of scanned hybrid metal–dielectric bullseye antenna array; (bottom) AFM writing tip is wetted, and a droplet of dilute QD suspension is placed at the center of each bullseye structure (guided by the image created in the first step), leaving behind a single QD.



# Electric Field Engineering to Unlock the Potential of Gallium Oxide Power Devices

Nolan Hendricks

Air Force Research Laboratory, Sensors Directorate

Gallium oxide ( $\text{Ga}_2\text{O}_3$ ) is an ultra-wide bandgap semiconductor with the potential to enable efficient power electronic devices beyond the wide bandgap revolution due to its estimated breakdown electric field of 8 MV/cm in addition to the availability of melt-grown substrates and multiple shallow donor species. However, the high breakdown electric field that enables the potential benefits brings its own challenges in device engineering to realize these benefits.

One of the principal power devices is the diode. Schottky diodes are typically preferred due to lower turn-on voltage and faster recovery times compared to p-n diodes. However, metal semiconductor junctions with barrier heights less than 2 eV are not capable of sustaining high electric fields due to the large magnitude of tunneling current and increased thermionic emission current. While larger Schottky barrier heights or p-n heterojunctions can offer better rectifying, they come at the cost of larger turn-on voltage. This work will show progress made in the integration of thin  $\text{TiO}_2$  interlayers in unipolar  $\text{Ga}_2\text{O}_3$  diodes. The negative conduction band offset of  $\text{TiO}_2$  relative to  $\text{Ga}_2\text{O}_3$  does not introduce an additional energy barrier to forward conduction, while the high permittivity reduces the electric field at the surface. As a result, this interlayer greatly reduces the leakage current and increases the breakdown voltage compared to standard Schottky diodes while maintaining low on-state losses. We will also show the incorporation of trench-MOS RESURF structures and NiO guard rings as additional electric field management tools to create diodes with high breakdown field, negligible leakage current, and low turn-on voltage.

Another challenge in engineering the electric field in  $\text{Ga}_2\text{O}_3$  is edge termination without p-type material. Multiple options are available, and this work will go over progress made in the use of NiO for guard rings and  $\text{BaTiO}_3$  as a high permittivity dielectric for field plates, each showing electric fields higher than is possible with unterminated structures.

These results will highlight the recent progress and ongoing research needs to deliver on the promises of figures of merit and realize efficient  $\text{Ga}_2\text{O}_3$  power devices with performance beyond the limits of current wide bandgap semiconductors.

# Study on Metal-Oxide Field Effect Transistors of $\beta$ -Gallium Oxide with AlGaO Spacer Layer for High Power Device Applications

Sheng-Ti Chung<sup>a</sup>, Bing-Hang Li<sup>a</sup>, Catherine Langpoklakpam<sup>b</sup>, Fu-Gow Tarntair<sup>a</sup>, Wei Hsiang Chiang<sup>c</sup>, Yi-Kai Hsiao<sup>d</sup>, Hao-Chung Kuo<sup>b,d</sup>, Dong Sing Wu<sup>c,e</sup>, Ray-Hua Horng<sup>a</sup>

<sup>a</sup> Institute of Electronics, National Yang Ming Chiao Tung University, Hsinchu 30010, Taiwan, ROC <sup>b</sup> Department of Photonics and Institute of Electro-Optical Engineering, College of Electrical and Computer Engineering, National Yang-Ming Chiao Tung University, Hsinchu 30010, Taiwan, ROC

<sup>c</sup> Department of Materials Science and Engineering, National Chung Hsing University,

Taichung 40227, Taiwan, ROC

<sup>d</sup> Hon Hai Research Institute, Semiconductor Research Center, Taipei 11492, Taiwan, ROC <sup>e</sup> Department of Applied Materials and Optoelectronic Engineering, National Chi Nan

University, Nantou 54561, Taiwan, ROC

**Abstract**—This study utilized metalorganic chemical vapor deposition (MOCVD) technology to grow  $\beta$ -Ga<sub>2</sub>O<sub>3</sub> epitaxial layers on sapphire substrates and fabricate lateral  $\beta$ -Ga<sub>2</sub>O<sub>3</sub> field-effect transistors (FETs). To enhance the performance of these FETs, a  $\beta$ -Ga<sub>2</sub>O<sub>3</sub>/(Al<sub>0.13</sub>Ga<sub>0.87</sub>)<sub>2</sub>O<sub>3</sub> structure was incorporated. The resulting FETs demonstrated high on-state current ( $I_{on}$ ), low on-state resistance ( $R_{on}$ ), and a high on-off ratio of drain current, indicating excellent two-dimensional electron gas (2DEG) characteristic offered by  $\beta$ -Ga<sub>2</sub>O<sub>3</sub>/(Al<sub>0.13</sub>Ga<sub>0.87</sub>)<sub>2</sub>O<sub>3</sub> structure. By optimizing the thickness and doping concentration of  $\beta$ -Ga<sub>2</sub>O<sub>3</sub>, high-performance 2DEG  $\beta$ -Ga<sub>2</sub>O<sub>3</sub> FETs were achieved, which satisfied the stringent requirements for power devices. Notably, the heavily doped  $\beta$ -Ga<sub>2</sub>O<sub>3</sub>/(Al<sub>0.13</sub>Ga<sub>0.87</sub>)<sub>2</sub>O<sub>3</sub> structure led to a significant improvement in performance, with the saturation current ( $I_{D,sat}$ ) increasing from 0.16 mA/mm to 11.4 mA/mm—a remarkable 6925% increase—and the breakdown voltage rising from 331 V to 687 V, an increase of 107.25%. The relative performance of device with and without AlGaO were also simulated. These enhancements were primarily due to the effective reduction of leakage current density and 2DEG formation by the  $\beta$ -Ga<sub>2</sub>O<sub>3</sub>/(Al<sub>0.13</sub>Ga<sub>0.87</sub>)<sub>2</sub>O<sub>3</sub> layer, which was grown by the importance of precise growth parameters and structural design in advancing the performance of  $\beta$ -Ga<sub>2</sub>O<sub>3</sub> FETs, making them highly promising for high-power applications.

**Index Terms**—Ga<sub>2</sub>O<sub>3</sub>, MOCVD, Two-Dimensional Electron Gas (2DEG), AlGaO, High Voltage.

## Computational design of optimal heterostructure materials for monoclinic Ga<sub>2</sub>O<sub>3</sub>

Hartwin Peelaers, Department of Physics and Astronomy, University of Kansas, Lawrence, KS, USA

Ga<sub>2</sub>O<sub>3</sub>, a wide-band gap semiconductor, is of interest for high-power devices and deep-UV photodetectors. Many of these applications require the formation of heterostructures to create a conduction-band offset to confine charge carriers. This is commonly achieved through alloying with Al<sub>2</sub>O<sub>3</sub>. However, Al<sub>2</sub>O<sub>3</sub> has a significantly smaller lattice constant than Ga<sub>2</sub>O<sub>3</sub>, which can introduce strain on the heterostructure. Experimentally, it has been difficult to grow Al<sub>2</sub>O<sub>3</sub>-Ga<sub>2</sub>O<sub>3</sub> alloys with high Al content, so that the maximum achieved conduction-band offset is only around 0.33eV. High Al containing alloys are also difficult to n-type dope.

We use hybrid density functional theory simulations to design a heterostructure which closely matches the lattice constant of Ga<sub>2</sub>O<sub>3</sub>, while maintaining a conduction-band offset. We found that alloys of In<sub>2</sub>O<sub>3</sub> and Al<sub>2</sub>O<sub>3</sub> form a lattice-matched monoclinic structure with a 1 eV conduction-band offset [1]. Moreover, we show that this alloy can readily be n-type doped using Si [2]. We will also discuss the role of charge-carrier compensation by cation vacancies in Al<sub>2</sub>O<sub>3</sub>-Ga<sub>2</sub>O<sub>3</sub> and In<sub>2</sub>O<sub>3</sub>-Al<sub>2</sub>O<sub>3</sub> alloys.

[1] S. Seacat, J.L. Lyons, and H. Peelaers, *Phys. Rev. Materials* 8, 014601 (2024).

[2] S. Seacat and H. Peelaers, *J. Appl. Phys.* 135, 235705 (2024).

# Combinatorial Synthesis and Physical Property Screening of Ternary Alloys of Rhombohedral $\alpha$ -Ga<sub>2</sub>O<sub>3</sub> and Transition Metal Sesquioxides

C. Petersen<sup>1,\*</sup>, S. Vogt,<sup>1</sup> M. Grundmann<sup>1</sup>, and H. von Wenckstern<sup>1</sup>

<sup>1</sup> Universität Leipzig, Felix Bloch Institute for Solid State Physics, Semiconductor Physics Group, Leipzig, Germany

\*E-mail: clemens.petersen@uni-leipzig.de

Due to its high band gap of 4.6-5.3 eV and high predicted breakdown field of 8 MV/cm [1], much attention is drawn to the ultra-wide band gap semiconductor Ga<sub>2</sub>O<sub>3</sub> for applications in high-power devices and solar blind optoelectronic devices. However, besides the well-studied thermodynamically stable monoclinic  $\beta$ -phase of Ga<sub>2</sub>O<sub>3</sub> the metastable  $\alpha$ -polymorph with corundum structure is gaining scientists interest more and more. Since it is isostructural to  $\alpha$ -Al<sub>2</sub>O<sub>3</sub>, miscibility over the entire composition range of  $\alpha$ -(Al<sub>x</sub>Ga<sub>1-x</sub>)<sub>2</sub>O<sub>3</sub> was reported [2] and the growth of  $\alpha$ -Ga<sub>2</sub>O<sub>3</sub> on cost-effective sapphire substrates is feasible, while maintaining high crystallinity [3]. To facilitate band gap engineering towards lower band gaps, various rhombohedral transition metal sesquioxides with similar lattice constants to  $\alpha$ -Ga<sub>2</sub>O<sub>3</sub> are available. Materials with band gaps in the UV-range, such as 3.3 eV for  $\alpha$ -Cr<sub>2</sub>O<sub>3</sub>, but also materials with band gaps in the infrared range down to 0.7 eV or 0.1 eV for  $\alpha$ -V<sub>2</sub>O<sub>3</sub> and  $\alpha$ -Ti<sub>2</sub>O<sub>3</sub> are of interest to form ternary or multinary alloys with  $\alpha$ -Ga<sub>2</sub>O<sub>3</sub>. The  $\alpha$ -(Me,Ga)<sub>2</sub>O<sub>3</sub> material system thus offers the possibility to tune the band gap from 8.8 eV ( $\alpha$ -Al<sub>2</sub>O<sub>3</sub>) down to 0.14 eV ( $\alpha$ -Ti<sub>2</sub>O<sub>3</sub>), e.g. for possible applications in wavelength-selective optoelectronics.

In this work, we showcase how combinatorial material synthesis by pulsed laser deposition [4] can be employed in combination with high-throughput physical property screening to rapidly characterize novel oxide material systems such as  $\alpha$ -(Me,Ga)<sub>2</sub>O<sub>3</sub>. Thus, we realized spatially addressable material libraries of (Cr<sub>x</sub>Ga<sub>1-x</sub>)<sub>2</sub>O<sub>3</sub>, (Ti<sub>x</sub>Ga<sub>1-x</sub>)<sub>2</sub>O<sub>3</sub>, and (V<sub>x</sub>Ga<sub>1-x</sub>)<sub>2</sub>O<sub>3</sub> thin films using continuous composition spread PLD over a large compositional range with high chemical resolution. The physical properties of the ternary material systems were screened by means of high-throughput spatially resolved X-ray diffraction (XRD), energy-dispersive X-ray spectroscopy (EDX), UV-VIS transmission and spectroscopic ellipsometry (SE) measurements. For all investigated material systems a comparison of the ternary material libraries properties to those of the binary reference systems is drawn to gain a profound understanding of the influence of the composition  $x$  in these oxide alloy systems. For (Cr<sub>x</sub>Ga<sub>1-x</sub>)<sub>2</sub>O<sub>3</sub> and (V<sub>x</sub>Ga<sub>1-x</sub>)<sub>2</sub>O<sub>3</sub>, phase-pure growth in the rhombohedral crystal structure could be demonstrated over the entire composition range, while for the (Ti<sub>x</sub>Ga<sub>1-x</sub>)<sub>2</sub>O<sub>3</sub> material library a miscibility limit of  $x = 25$  at.% within the  $\alpha$ -structure is found. A significant red shift of the absorption edge with increasing  $x$  was found for all investigated material libraries. These findings demonstrate the feasibility of the  $\alpha$ -(Me,Ga)<sub>2</sub>O<sub>3</sub> material systems for bandgap engineering over an exceptionally large energy range without phase-separation. Furthermore, this work demonstrates how insight into complex alloy material systems can be gained with otherwise inaccessible efficiency and experimental throughput by employing combinatorial material synthesis.

[1] M. Higashiwaki, K. Sasaki, A. Kuramata, Appl. Phys. Lett., Vol. 100, 013504 (2012)

[2] A. Hassa, P. Storm, M. Kneiß, physica status solidi (b), Vol. 258, No. 2, 2000394 (2020)

[3] C. Petersen, S. Vogt, M. Kneiß, APL Materials, Vol. 11, No. 6, 061122 (2023)

[4] H. von Wenckstern, M. Kneiß, A. Hassa, physica status solidi (b), Vol. 257, No. 7, 1900626 (2019)

## Metal-Semiconductor Interfaces and Ohmic Contacts on $\beta$ -Ga<sub>2</sub>O<sub>3</sub>

Kathleen T. Smith<sup>1</sup>, Naomi Pieczulewski<sup>2</sup>, Cameron A. Gorsak<sup>2</sup>, Joshua T. Buontempo<sup>2</sup>, Michael O. Thompson<sup>2</sup>, Debdeep Jena<sup>2,3,4</sup>, Hari P. Nair<sup>2</sup>, Huili Grace Xing<sup>2,3,4</sup>

<sup>1</sup>School of Applied and Engineering Physics, Cornell University, Ithaca, NY 14853, USA

<sup>2</sup>Department of Materials Science and Engineering, Cornell University, Ithaca, NY 14853, USA

<sup>3</sup>School of Electrical and Computer Engineering, Cornell University, Ithaca, NY 14853, USA

<sup>4</sup>Kavli Institute at Cornell for Nanoscale Physics, Cornell University, Ithaca, NY 14853, USA

Metal-semiconductor contacts, and by extension metal-semiconductor interfaces, are a critical device building block. Oxide semiconductor-metal junctions present their own unique challenges and characteristics. Here we examine some of the nuances of these junctions through the lens of  $\beta$ -Ga<sub>2</sub>O<sub>3</sub>, an ultra-wide bandgap ( $\sim 4.8$  eV) semiconductor with potential applications in high voltage power electronics due to a large critical electric field, large Baliga's figure of merit, demonstrated range of n-type doping, and relative feasibility of native substrates.

Low resistance ohmic contacts, especially to wide and ultra-wide bandgap oxides, have historically relied on a combination of low work function metals (such as Ti) and rapid-thermal annealing to encourage oxidation of the contact metal, forming an intermediate semiconductor layer. However, ohmic contacts to  $\beta$ -Ga<sub>2</sub>O<sub>3</sub> have suffered from poor repeatability and consistency. In the first section of this talk, we examine standard ohmic contact processes and demonstrate that even single monolayer carbon contamination from lithography during conventional liftoff processes can significantly impede ohmic contact formation. While metal-first contact processing avoids this added contamination, adventitious carbon from air exposure prior to sample fabrication is demonstrated to have a measurable impact on contact resistance. Organic cleaning procedures such as active oxygen descums and UV-ozone are demonstrated to remove both lithographic carbon contamination and adventitious carbon residue when performed for sufficient time, resulting in as-deposited 0.05  $\Omega$ -mm contacts fabricated both by liftoff and metal-first processes without the need for an alloying anneal. These results highlight the need for careful control of interface contaminants in metal-oxide semiconductor contact systems.

In the second section of this talk, we apply the contact processing improvement developed for Ti-based ohmic contacts to the broader question of Fermi-level pinning in metal contacts to  $\beta$ -Ga<sub>2</sub>O<sub>3</sub>. Historical Schottky barrier height measurements with a wide range of work functions have not shown the linear dependence on metal work function predicted by the Schottky-Mott rule, indicating a largely pinned interface. To address this question, we develop a refined version of the thermionic field emission model to describe the Schottky barrier height for low-work function metals by relating contact resistance and barrier height. We then fabricated a series of test structures having a range of contact metal work functions using the metal-first process to avoid the above-mentioned interface contamination. The resulting Schottky barriers showed a largely monotonic dependence on the contact metal work function with a surface index of behavior of  $\sim 0.7$ , indicating significant alleviation of Fermi-level pinning. Further investigations of the as-deposited interface chemistry by depth-resolved XPS indicates that low work function metals readily getter oxygen from the underlying  $\beta$ -Ga<sub>2</sub>O<sub>3</sub> at room temperature, forming higher work function metal oxide contact layers, which explains the mild residual Fermi level pinning. Overall, this work demonstrates that interface carbon contamination and spontaneous interface oxidation are significant contributors to oxide contact behavior.

## **Ion Beam Synthesis of Layer-Tunable and Transfer Free Graphene for Device Applications**

Yongqiang Wang<sup>1</sup>, Gang Wang<sup>2</sup>, and Caichao Ye<sup>3</sup>

<sup>1</sup> Los Alamos National Laboratory, Los Alamos, NM, USA

<sup>2</sup> Ningbo University, Ningbo, Zhejiang, China

<sup>3</sup> Southern University of Science and Technology, Shenzhen, Guangdong, China

Direct synthesis of layer-tunable and transfer-free graphene on technologically important substrates is highly valued for various electronics and device applications. State of the art in the field is currently a two-step process: a high-quality graphene layer synthesis on metal substrate through chemical vapor deposition (CVD) followed by delicate layer-transfer onto device-relevant substrates. Here, we report a novel synthesis approach combining ion implantation for a precise graphene layer control and dual-metal smart Janus substrate for a diffusion-limiting graphene formation, to directly synthesize large area, high quality, and layer-tunable graphene films on arbitrary substrates without the post-synthesis layer transfer process.

Carbon (C) ion implantation was performed on Cu-Ni film deposited on a variety of device-relevant substrates. A well-controlled number of layers of graphene, primarily monolayer and bilayer, is precisely controlled by the equivalent fluence of the implanted C-atoms (1 monolayer  $\sim 4 \times 10^{15}$  C-atoms/cm<sup>2</sup>). Upon thermal annealing to promote Cu-Ni alloying, the pre-implanted C-atoms in the Ni layer are pushed towards the Ni/substrate interface by the top Cu layer due to the poor C-solubility in Cu. As a result, the expelled C-atoms precipitate into graphene structure at the interface facilitated by the Cu-like alloy catalysis. After removing the alloyed Cu-like surface layer, the layer-tunable graphene on the desired substrate is directly realized.

This presentation will focus on graphene layer formation mechanism, detailed characterizations, and performance characteristics of select devices fabricated through this ion beam approach.

LA-UR-24-23745

# **Study of interfacial properties of Ti/ Ga<sub>2</sub>O<sub>3</sub> Schottky junctions processed with SiH<sub>4</sub> plasma**

Sahyadri Patil<sup>(a)</sup> and Mengbing Huang

Department of Nanoscale Science and Engineering, University at Albany, 257 Fuller Road,  
Albany, NY12203, USA

<sup>(a)</sup> Email address: spatil@albany.edu

$\beta$ -Gallium Oxide ( $\beta$ -Ga<sub>2</sub>O<sub>3</sub>) has been considered a promising material for next- generation power electronics due to its ultra-wide bandgap of 4.6-4.9 eV. Despite the excellent material properties of  $\beta$ -Ga<sub>2</sub>O<sub>3</sub>, the performance of metal-Ga<sub>2</sub>O<sub>3</sub> contacts may hinder its applications in advanced power electronics. It remains a challenge to achieve ohmic contacts and Schottky junctions with good electrical performance and thermal stability in  $\beta$ -Ga<sub>2</sub>O<sub>3</sub> due to complicated surface defects and metal-semiconductor interfacial reactions. In this study, we investigate the effects of SiH<sub>4</sub> plasma treatment on Fe-doped semi-insulating  $\beta$ -Ga<sub>2</sub>O<sub>3</sub> surfaces, focusing on its impact on the chemistry and electronic properties at the interface formed by depositing a thin Ti film on  $\beta$ -Ga<sub>2</sub>O<sub>3</sub> surfaces. The study has been aided with detailed x-ray photoelectron spectroscopy (XPS) characterizations of Ga/O stoichiometry, O vacancy, surface band bending, and Ti/Ga<sub>2</sub>O<sub>3</sub> Schottky barrier. The analyses reveal an apparent increase in oxygen vacancy concentration in the  $\beta$ -Ga<sub>2</sub>O<sub>3</sub> surface following 5-nm Ti thin film deposition, with a much stronger effect caused by the SiH<sub>4</sub> plasma treatment. The passivation of vacancy defects in the plasma-treated sample is evidenced by an increase in binding energy relative to the case without plasma treatment. While the SiH<sub>4</sub> plasma treatment significantly increases the downward surface band bending ( $\sim 1.17$  eV) as opposed to the control sample ( $\sim 0.67$  eV), the Schottky barrier heights remain almost the same in both cases ( $\sim 1.36$  vs.  $\sim 1.42$  eV). Angle-resolved XPS measurements on the Ti/Ga<sub>2</sub>O<sub>3</sub> samples suggest that a TiO<sub>2</sub> layer is formed at the Ti/Ga<sub>2</sub>O<sub>3</sub> interface, with its thickness limited by the plasma treatment. These findings will be discussed to understand the plasma effects on  $\beta$ -Ga<sub>2</sub>O<sub>3</sub> surface defects and provide insights to engineer metal/Ga<sub>2</sub>O<sub>3</sub> contacts with plasma-induced surface/interface modifications.

**Wednesday**  
**03/05/2025**



# Formation of strain relaxed thin ( $<30\text{nm}$ ) epitaxial $\text{Si}_{1-x}\text{Ge}_x$ layers on a silicon substrate via ion implantation and selective oxidation

Andrew P. Knights<sup>\*1</sup>, Ross Anthony<sup>1</sup>, Yaser Haddara<sup>2</sup>, Arezoo Mafi<sup>1</sup>, Sunzhuoran Wang<sup>1</sup>, Pooya Torab Ahmadi<sup>1</sup>, Trevor Smith<sup>1</sup>, Spencer McDermott<sup>1</sup>, Sophie Bierer<sup>1</sup>, Chengqian Liao<sup>1</sup>, Bruno Segat Frare<sup>1</sup>, Jonathan D.B. Bradley<sup>1</sup>, and Ryan B. Lewis<sup>1</sup>

<sup>1</sup> Department of Engineering Physics, McMaster University, L8S 4L7 Hamilton, Canada

<sup>2</sup> Department of Electrical and Computer Engineering, McMaster University L8S 4L7 Hamilton, Canada

\*aknight@mcmaster.ca

We show that an ultra-thin  $\text{Si}_{1-x}\text{Ge}_x$  layer fabricated by an oxidative solid-phase epitaxy process can facilitate efficient strain relaxation, where germanium condensation is used to create the thin film, utilizing a wet oxidation process. Both silicon and silicon-on-insulator samples were implanted with a fluence of  $3$  or  $5 \times 10^{16} \text{ cm}^{-2}$   $\text{Ge}^+$  at an energy of  $30$ ,  $33$  or  $35\text{keV}$ . In some cases, a primary post-implantation wet oxidation was performed initially at  $870$  degrees C for  $70$  min, with the aim of capping the sample without causing significant dose loss via Ge evaporation through the sample surface. This was followed by a secondary higher temperature wet oxidation at either  $900$  degrees C,  $1000$  degrees C, or  $1080$  degrees C. In other cases, a single oxidation step at  $900$  degrees C for  $30$  minutes was used. The germanium retained dose and concentration profile, and the oxide thickness is examined after primary oxidation, and various secondary oxidation times, using Rutherford backscattering analysis. A mixed SiGe oxide is observed to form during the primary oxidation followed by a pure silicon oxide after higher temperature secondary oxidation. The germanium layer formed beneath the  $\text{SiO}_2$  layer is crystalline in nature and seeded by the underlaying silicon, confirmed by transmission electron microscopy. It is also observed that both the diffusion of germanium and the rate of oxidation are enhanced at  $870$  and  $900$  degrees C compared to equilibrium expectations. To elucidate the physical mechanisms, which govern the implantation-condensation process, we fit the experimental profiles of the samples with a model that uses a modified segregation boundary condition; a modified linear rate constant for the oxidation; and an enhanced diffusion coefficient of germanium where the enhancement is inversely proportional to the temperature and decays with increasing time [1]. The germanium rich layer is essentially strain relaxed. The efficient strain relaxation results from the high oxidation temperature, producing a periodic network of dislocations at the substrate interface. Preliminary growth of epitaxial GaAs is performed on the relaxed  $\text{Si}_{1-x}\text{Ge}_x$  layer, demonstrating a promising new pathway for integrating III-V lasers directly on the Si platform [2].

[1] R Anthony et al., Jnl. of Appl. Phys., 122, (2017) article i.d. 065306.

[2] T R Smith et al., Advanced Mat. Int., (2024) early access i.d. 2400580.

# **Cryogenic Performance of $\text{In}_{0.8}\text{Ga}_{0.2}\text{As}$ Quantum-Well HEMTs:**

## **Scaling Limits and High-Frequency Operation**

Tae-Woo Kim

*Department of Electrical and Computer Engineering, Texas Tech University, Texas*

As quantum computing transitions from fundamental research to large-scale practical implementation, the demand for high-performance cryogenic electronics is rapidly increasing. Modern superconducting quantum processors require precise control and readout electronics operating at deep cryogenic temperatures ( $\sim 4$  K or below). However, as quantum computers scale from hundreds to thousands of qubits, the associated power dissipation and signal integrity challenges become critical. This necessitates the development of ultra-low-power, high-frequency transistors that can function efficiently at cryogenic temperatures while maintaining low noise, high gain, and minimal power dissipation ( $< 1$  mW per transistor).

In this study, we investigate the scaling behavior and cryogenic performance of  $\text{In}_{0.8}\text{Ga}_{0.2}\text{As}$  quantum-well high-electron-mobility transistors (HEMTs), fabricated with gate lengths ( $L_g$ ) ranging from 10  $\mu\text{m}$  to 30 nm and evaluated from 300 K down to 4 K. The fabricated 30 nm gate-length device, optimized for cryogenic operation, achieves record-breaking DC and RF performance, with  $g_{m,\text{max}} = 2.6$  mS/ $\mu\text{m}$ ,  $R_{\text{ON}} = 349$   $\Omega \cdot \mu\text{m}$ , and cutoff frequencies of  $f_T = 732$  GHz and  $f_{\text{max}} = 700$  GHz at 4 K—setting a new benchmark in cryogenic FET technology.

Through detailed carrier transport analysis, we observe a significant enhancement in effective mobility ( $\mu_{\text{eff}}$ ) from 12,200  $\text{cm}^2/\text{V} \cdot \text{s}$  at 300 K to 23,000  $\text{cm}^2/\text{V} \cdot \text{s}$  at 4 K, while the saturation velocity ( $v_{\text{sat}}$ ) improves from  $4.6 \times 10^7$  cm/s to  $5.1 \times 10^7$  cm/s. Delay-time decomposition attributes the high  $f_T$  at cryogenic temperatures to the combined effects of reduced source resistance ( $R_s$ ) and enhanced intrinsic transconductance ( $g_{\text{mi}}$ ), highlighting the superior electron transport properties of InGaAs in low-temperature environments. Additionally, negative differential output conductance (NDOC) effects are observed below 50 K, emphasizing the unique transport dynamics of these transistors at extreme temperatures.

The results presented in this work establish InGaAs QW HEMTs as a key enabling technology for next-generation cryogenic electronics, addressing critical needs in quantum computing, deep-space communication, and ultra-low-noise amplifiers (CLNA). With the first demonstration of simultaneous  $f_T$  and  $f_{\text{max}}$  exceeding 700 GHz in any cryogenic FET, this work paves the way for highly scalable, energy-efficient quantum readout and control architectures crucial for the future of quantum computing and THz-speed communication.

## **Visualization of polarization induced phonons in ferroelectric oxides**

**Sandhya Susarla**

**Arizona State University**

Ferroelectric materials, which maintain polarization without an electric field, are promising for low-power computing and memory applications. The strong coupling between spin, lattice, orbital, and charge degrees of freedom in these materials results in the energetically equivalent polar regions known as “domains” and subsequently domain walls (DWs) that separate two domains. There are unique logic devices envisioned around engineering domains and DWs. A complete understanding of the electronic and phononic properties, which influence information transfer and heat dissipation, is essential to realize such devices. In this talk, I will explain differential momentum resolved STEM-EELS, a technique that my team is developing at ASU to observe polarization induced phonons. We observe that these phonons modes change in the c and a domains in  $\text{PbTiO}_3$  and strongly correlated with the local crystal field splitting. This technique can potentially be extended to other type of ferroelectric materials such as hafnia, and rare earth manganates.

# **Transparent Hybrid Electrodes for Next-Generation Flexible Photovoltaic Applications**

**Terry Alford**

**Arizona State University**

Transparent conductive oxides (TCOs) are extensively utilized as electrodes in organic photovoltaic (OPV) devices and organic light-emitting diode (OLED) devices. Recently, flexible and transparent composite electrodes (TCEs), particularly TCO/metal/TCO multilayers, have garnered significant attention due to rapid advancements in flexible optoelectronics, including OPVs, flat-panel displays, and next-generation flexible OLEDs. TCEs fabricated on flexible substrates are especially compelling due to their flexibility, durability, lightweight nature, and potential for portability. Since the performance of flexible optoelectronic devices is highly dependent on electrode quality, developing high-quality flexible TCEs with low resistivity, high transparency, and excellent mechanical flexibility is crucial. This presentation explores key challenges related to low-temperature processing, microstructure, and these composite structures' electrical and optical properties.

# Correlations between the growth conditions of homoepitaxially grown $\beta$ -Ga<sub>2</sub>O<sub>3</sub> and their structural, optical and transport properties

J.-M. Chauveau<sup>1a)</sup>, S.L. Park<sup>2</sup>, Z. Chi<sup>1</sup>, C. Sartel<sup>1</sup>, M. Fregnaud<sup>3</sup>, Y. Zheng<sup>4</sup>, S. Douglas<sup>5</sup>, L. Penman<sup>5</sup>, F. Massabuau<sup>5</sup>, A. Amador Perez tomas<sup>6</sup>, S.M. Koo,<sup>2</sup> and Ekaterine Chikoidze<sup>1</sup>

<sup>1</sup>Université Paris-Saclay, UVSQ, CNRS, GEMaC, 45 Av. des Etats-Unis, 78035, Versailles Cedex, France

<sup>2</sup>Department of Electronic Materials Engineering, Kwangwoon University, Seoul 01897, Republic of Korea

<sup>3</sup>Université Paris-Saclay, UVSQ, CNRS, ILV, 45 Av. des Etats-Unis, 78035 Versailles Cedex, France

<sup>4</sup>Sorbonne Université, CNRS, INSP, 4 place Jussieu, 75252 Paris, France

<sup>5</sup>Department of Physics, SUPA, University of Strathclyde, Glasgow, G4 0NG, UK

<sup>6</sup>The Institute of Microelectronics of Barcelona CSIC CNM, Campus UAB, Bellaterra, 08193 Barcelona, Spain

<sup>a)</sup> Electronic mail: Jean-Michel.Chauveau@uvsq.fr

The material gallium oxide (Ga<sub>2</sub>O<sub>3</sub>) has recently attracted significant attention from researchers and industries due to its promising electronic properties, including a wide bandgap, a high breakdown field, carrier concentration control, and high thermal stability. These properties position gallium oxide as a potentially promising candidate for utilization in high-power electronic devices. However, *p*-type doping remains a primary challenge for this emerging technology. A range of approaches have been proposed to address this challenge; however, these approaches are all impeded by the substantial activation energies of the potential acceptors. Furthermore, a comprehensive understanding of the native defect creation and their electronic properties in  $\beta$ -Ga<sub>2</sub>O<sub>3</sub> is imperative to achieve efficient doping properties<sup>1,2</sup>.

The present study investigates the correlations between the O/Ga ratios during the homoepitaxial growth of  $\beta$ -Ga<sub>2</sub>O<sub>3</sub> and the structural and electrical properties thereof.

Homoepitaxial non-intentionally doped  $\beta$ -Ga<sub>2</sub>O<sub>3</sub> thin films were grown on Fe-doped (-201)  $\beta$ -Ga<sub>2</sub>O<sub>3</sub> substrates via metal-organic chemical vapor deposition (MOCVD) with varying O/Ga ratios. The structural properties of the samples were systematically investigated by X-ray diffraction (XRD), X-ray photoelectron spectroscopy (XPS), and atomic resolution scanning electron transmission microscopy (STEM). It was observed that there was a drastic improvement in the structural properties with an increase in the O/Ga ratio, as evidenced by the decrease in the full width at half maximum (FWHM) of the XRD peaks, better stoichiometry, and a decrease in the oxygen vacancies, as indicated by the XPS results. The enhancement of the structural properties was further confirmed through photoluminescence analysis, where a strong quenching of the luminescence was observed as the O/Ga ratio decreased. This quenching is indicative of an increased non-radiative recombination rate, which may be indicative of an increased concentration of non-radiative recombination centers within the sample, or a reduced concentration of donor/acceptor states available for trapping/retrapping of carriers.

A bespoke configuration was engineered to investigate electrical transport measurements of high-impedance samples. The temperature-dependent Hall effect measurements were conducted across a temperature range extending from 300 to 850 K, under 1.6 T. The investigation revealed that at elevated temperatures, the Hall hole concentrations for samples grown with high O/Ga ratios exhibited three orders of magnitude higher free hole concentrations compared to samples characterized by low O/Ga ratios. The origin of the measured carrier activation energies will be discussed.

<sup>1</sup>E. Chikoidze *et al.*, Materials Today Physics **3**, 118 (2017). <sup>2</sup>E. Chikoidze *et al.*, Journal of Materials Chemistry C **7**, 10231 (2019).

## **Artificial intelligence for on-the-fly analysis and control during oxide molecular beam epitaxy**

Tiffany Kaspar<sup>1</sup>, Emily Saldanha<sup>2</sup>, Henry Sprueill<sup>2</sup>, Jenna Pope<sup>2</sup>, Sarah Akers<sup>2</sup>, Derek Hopkins<sup>3</sup>, Ethan King<sup>2</sup>

<sup>1</sup>Physical and Computational Sciences Directorate, Pacific Northwest National Laboratory, P.O. Box 999, Richland, WA 99352

<sup>2</sup>National Security Directorate, Pacific Northwest National Laboratory, P.O. Box 999, Richland, WA 99352

<sup>3</sup>Earth and Biological Sciences Directorate, Pacific Northwest National Laboratory, P.O. Box 999, Richland, WA 99352

Modern synthesis methods enable the fabrication of an ever-expanding array of novel, non-equilibrium, and/or metastable materials that may possess unique and desirable functionality. Thin film deposition by molecular beam epitaxy (MBE) can produce atomically precise (or nearly so) materials with a wide range of functional electronic, magnetic, ferroelectric/multiferroic, optical, and/or ion-conducting properties. We are working to employ artificial intelligence (AI)-accelerated analysis of in situ and ex situ data streams for on-the-fly feedback control of the MBE deposition process that will enable targeted synthesis of novel materials with desired structure and functional properties. This in situ feedback control is a critical component of autonomous experimentation (AE), which promises orders-of-magnitude acceleration of materials discovery, optimization, and adoption in advanced technologies. The same AE approaches that accelerate materials discovery can also be applied in production environments to increase yield and reproducibility, saving time and energy. Here we present a machine-learning-enabled framework for analysis of reflection high energy electron diffraction (RHEED) pattern images in real time (one image per second). We demonstrate this framework using RHEED images collected from the deposition of epitaxial oxide thin films such as anatase TiO<sub>2</sub> on SrTiO<sub>3</sub>(001). Advantages and disadvantages of our approach will be discussed, as well as our efforts towards on-the-fly feedback control of MBE deposition parameters.

# Structural and Optical Analyses of Ytterbium Implantation-Induced Effects and Defects in $\beta$ -Ga<sub>2</sub>O<sub>3</sub>

R. Ratajczak<sup>1</sup>, J. Matulewicz<sup>1</sup>, M. Sarwar<sup>2</sup>, V. Ivanov<sup>2</sup>, D. Kalita<sup>1</sup>, E. Grzanka<sup>3</sup>, C. Mieszczyński<sup>1</sup>, P. Józwiak<sup>1</sup>, U. Kentsch<sup>4</sup>, R. Heller<sup>4</sup> and E. Guzewicz<sup>2</sup>

<sup>1</sup> National Centre for Nuclear Research, Soltana 7, 05-400 Otwock, Poland

<sup>2</sup> Inst. of Physics, Polish Acad. of Sciences, Aleja Lotników 32/46, 02-668 Warsaw, Poland

<sup>3</sup> Institute of High Pressure Physics, Polish Acad. of Sciences, Sokółowska 29/37, 01-142 Warsaw, Poland

<sup>4</sup> Helmholtz-Zentrum Dresden-Rossendorf, Bautzner Landstrasse 400 D-01328 Dresden, Germany

Rare earth (RE) doped gallium oxide, especially in its stable beta form ( $\beta$ -Ga<sub>2</sub>O<sub>3</sub>), has great potential for future use in optoelectronic devices. This is because, with the addition of RE ions into wide bandgap oxide materials, the base-light emission of the matrix can be optically tuned to the visible spectral range. Hence, the  $\beta$ -Ga<sub>2</sub>O<sub>3</sub>:RE systems seem attractive in applications such as phosphors, displays, high-power LEDs and high-end photodetectors, that can operate even in harsh environments. A crucial task in this field today is the development of controlled methods for doping this material.

One of the attractive ways to produce  $\beta$ -Ga<sub>2</sub>O<sub>3</sub>:RE systems is the ion implantation technique. However, due to the ballistic nature of the process, crystal lattice defects are formed. Created damage quenches the luminescence and makes a shorter lifetime of devices based on defected material. Thus, the annealing leading to the crystal recovery is required. The type of thermal treatment highly influences the structural and optical properties of the material.

In the current research, we paid particular attention to the issue of Yb-ion radiation-induced defects in the differently oriented  $\beta$ -Ga<sub>2</sub>O<sub>3</sub>:RE crystals, the structure recovery after different thermal treatments, and the optical response of Yb ions to these structural changes as well. To understand the nature of the defects and other observed effects, complementary analytical techniques such as HRXRD, HRTEM, and RBS/c were used, supported by Monte Carlo-based computer simulations code called *McChasy*<sup>1</sup>.

Our findings reveal pronounced structural and optical anisotropy. Notably, the (010)-oriented crystals exhibit a significantly reduced tendency to develop extended defects and are characterized by compressive stress. In contrast, the samples with the other two orientations exhibit tensile stress and a few times higher levels of extended defects. Interestingly, the PL spectra of (010)-oriented  $\beta$ -Ga<sub>2</sub>O<sub>3</sub> show the weakest emission from Yb<sup>3+</sup> ions. The results suggest the specific type of extended defects, whose creation is preferable in the other two orientations more than in (010) enhance Yb<sup>3+</sup> luminescence instead of suppressing it.

## References

[1] P. Józwiak et al *Nucl. Instrum. Methods Phys. Res. B.* **538**, 198 (2023)

## Acknowledgments

This research was carried out under the NCN project UMO-2022/45/B/ST5/02810 supported by Helmholtz Zentrum Dresden Rossendorf projects (23003447-ST, 23003449-ST).

# Room-temperature cavity-polaritons in planar ZnO microcavities fabricated via a top-down process using bulk ZnO single crystals

**K. Shima, K. Furusawa, and S. F. Chichibu**

*IMRAM-Tohoku Univ., 2-2-1 Katahira, Aoba-ku, Sendai, Miyagi 980-8577, Japan*

e-mail: [kshima@tohoku.ac.jp](mailto:kshima@tohoku.ac.jp)

Observations of the strong coupling of light with excitons in semiconductor microcavities (MCs) have attracted attention since it leads to the formation of bosonic quasi-particles, namely cavity polaritons. Because the effective mass of cavity polaritons is far smaller than that of free carriers or excitons, the realization of coherent light sources with ultra-low threshold current density based on Bose-Einstein condensation of cavity polaritons has been predicted.<sup>[1]</sup> Excitons in ZnO are stable at room temperature on the basis of their large binding energy (59 meV),<sup>[2]</sup> and thereby, polaritons in ZnO MCs have a huge Rabi-splitting energy ( $\Omega_{\text{Rabi}}$ ).<sup>[3]</sup> Therefore, ZnO is a preferred choice as an active layer material for polariton lasers that are operatable at room temperature. Recently, lasing actions of the ZnO MCs have been reported using semiconductor/dielectric hybrid distributed Bragg reflectors (DBRs)<sup>[4]</sup> and fully dielectric DBRs.<sup>[5]</sup> However, it is still challenging to combine the high crystalline quality of the large-area (millimeter-scale) ZnO active layer with the high photonic quality of the DBRs.  $\Omega_{\text{Rabi}}$  values for the ZnO MCs measured by photoluminescence (PL) and reflectance measurements have been as large as 130 meV,<sup>[6]</sup> which was smaller than the ideal value of 191 meV.<sup>[3]</sup> Possible reasons limiting  $\Omega_{\text{Rabi}}$  include insufficient reflectivity or stopband width of the mirrors and/or insufficient radiative performance of the ZnO active layer.

In this study, detection-angle-dependent energy shifts in the near-band-edge emission peak were observed at room temperature in planar ZnO MCs fabricated by a top-down process that simultaneously maintains the high radiative performance of the ZnO active layer and high-reflectivity of wide-bandwidth DBRs.<sup>[7]</sup> An approximately  $2\lambda$ -thick ZnO active layer with a thickness gradient of 67 nm/mm (i.e., an angle of gradient of 14 arcseconds) over the entire  $10 \times 5 \text{ mm}^2$  area was formed by thinning a bulk ZnO single crystal grown by the hydrothermal method, of which typical threading dislocation densities were lower than  $10^2 \text{ cm}^{-2}$ . The DBRs consisting of 10 and 12 pairs of  $\text{SiO}_2/\text{ZrO}_2$  multilayers were deposited as the top and bottom mirrors of the MCs, respectively, by nearly surface-damage-free reactive helicon-wave-excited-plasma sputtering method.<sup>[8]</sup> The quality factor of a passive cavity consisting of the same DBR stacks ranged from 670 to 720 for a large area of 1 mm in diameter. Angle-resolved PL spectra of the ZnO MCs measured at different positions with a macroscopic spot being 80  $\mu\text{m}$  in diameter exhibited distinct emissions from the lower branch of cavity-polaritons with apparent detunings ranging from -40 meV to 40 meV at room temperature. The results showed our planar ZnO MCs certainly exhibited a strong exciton-photon coupling regime at room temperature, which is a major step toward the realization of room-temperature polariton lasers.

This work was supported in part by Crossover Alliance and JSPS KAKENHI (Nos. 22246037, 17H06514, and 19K15453) under MEXT and Canon Foundation, Japan.

[1] A. Imamoglu *et al.*, PRA **53**, 4250 (1996). [2] D. G. Thomas, JPCS **15**, 86 (1960). [3] S. F. Chichibu *et al.*, SST **20**, S67 (2005). [4] J. R. Chen *et al.*, Opt. Express **19**, 4101 (2011). [5] F. Li *et al.*, PRL **110**, 196406 (2013). [6] Y. Y. Lai *et al.*, Sci. Rep. **6**, 20581 (2016). [7] K. Shima, K. Furusawa, and S. F. Chichibu, APL **117**, 071103 (2020). [8] S. F. Chichibu *et al.*, APL **88**, 161914 (2006).

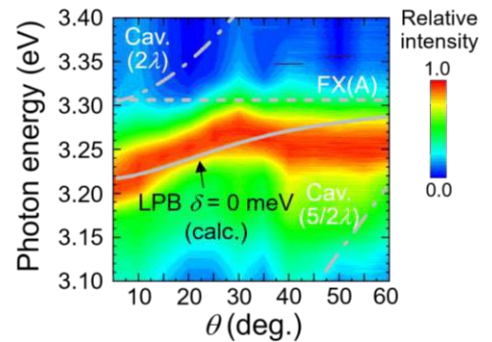


Fig. 1. Intensity color maps for the angular dispersions of the PL spectra of the ZnO MC at room temperature.



# Towards autonomous synthesis and characterization of oxide semiconductors and devices

Davi Febba, Stephen Schaefer, Brooks Tellekamp, Hilary Egan, William Callahan, Kingsley Egbo,  
Andriy Zakutayev

National Renewable Energy Laboratory (NREL), Golden, CO 80401, USA

Growth and characterization of thin film materials require long experimental campaigns to tune the processing conditions until desired material properties and chemical composition are achieved. If devices are under study, the cycle of synthesis, characterization and optimization is stretched even further, since now phenomena occurring at the materials interfaces play a significant role.

In this context, autonomous experimentation is transforming the landscape of synthesis and characterization of materials and devices. The incorporation of automation of repetitive tasks and artificial intelligence techniques to plan experiments based on the available data accelerate the materials discovery chain while minimizing human intervention, freeing researchers to focus on more strategically relevant tasks.

In this presentation, I will discuss the progress on autonomous experimentation at NREL for MBE synthesis of oxide semiconductors<sup>1</sup> and characterization of oxide-based devices in extreme environmental conditions<sup>2</sup>, enabled by automated instruments driven by artificial intelligence algorithms. These systems, equipped with sophisticated capabilities such as genetic algorithms, computer vision, and multidimensional Bayesian analysis, actively learn from data to efficiently identify the most informative data points. By leveraging these capabilities, they maximize the extraction of relevant information in a time-efficient manner, significantly reducing the need for manual intervention.

I will also address the challenges and solutions involved in adapting existing laboratory infrastructure to support autonomous workflows. Key efforts include instrument automation, workflow orchestration, data management, software development, and the establishment of subnetworks to enable seamless communication between remote servers and command-and-control computers.

1. Schaefer, S. *et al.* Rapid screening of molecular beam epitaxy conditions for monoclinic (In<sub>x</sub>Ga<sub>1-x</sub>)<sub>2</sub>O<sub>3</sub> alloys. *J. Mater. Chem. A* (2024) doi:10.1039/D3TA07220G.
2. Febba, D., Egbo, K., Callahan, W. A. & Zakutayev, A. From text to test: AI-generated control software for materials science instruments. *Digital Discovery* **4**, 35–45 (2025).

## Thermochromic Property of Sandwiched VO<sub>2</sub> Thin Films in Dielectric Layers

Jazmyne Smith, Alexis Neathery, Abdennaceur Karoui, and A.Victor Adedeji

*Elizabeth City State University, Elizabeth City, NC 27909*

The thermochromic characteristics of Vanadium dioxide (VO<sub>2</sub>) has been well investigated and reported. Vanadium dioxide (VO<sub>2</sub>) is a promising material for energy-saving smart windows and Radiative Cooling applications due to its reversible Metal-to-Insulator Transition (MIT), accompanying large and reversible changes in its optical, electrical and structural properties. The observed transition occurs at an easily accessible temperature of 68°C. The transformation from low-temperature monoclinic (M1) to high temperature rutile (R) structure is dramatic. The observed phase transitions in VO<sub>2</sub> have been stimulated thermally, electrically or optically. Pure vanadium metal thin films were deposited on crystalline quartz substrates by magnetron sputtering method and oxidized in 0.23% oxygen in pure N<sub>2</sub>/O<sub>2</sub> annealing gas mixture at 500°C furnace temperature, 800 mtorr pressure for four hours. The resulting VO<sub>2</sub> was sandwiched in insulating TaSiN or Ga<sub>2</sub>O<sub>3</sub>:Fe layers to abate observed corrosion that degrades sputtered VO<sub>2</sub> thin films characteristics after a few months sitting at ambient lab conditions. Transmittance spectrum data and the electrical transport characteristics showed that the hash process of oxidation of Vanadium thin films does not adversely affect the protective layer and VO<sub>2</sub> characteristics were not degraded by the insulating protective layers. The changes in transmittance and conductivity at transition temperature are larger for sandwiched VO<sub>2</sub> compared to the unprotected layer. The study of interfacial interactions between VO<sub>2</sub> and protective dielectric layers is essential to enhance the quality of the switching and preserve it over a long period of time.

# **VO<sub>2</sub> Phase Transition-Based Oscillators for Oscillatory Neural Networks**

Yinxuan Qiao, Zhaoyang (Frank) Fan

School of Electrical, Computer and Energy Engineering, Arizona State University, Tempe, AZ 85281, USA

VO<sub>2</sub>-based oscillators have gained significant attention in neuromorphic computing due to their insulator-to-metal transition (IMT), which enables self-sustained and tunable oscillations. These oscillators mimic the spiking behavior of biological neurons, making them a promising building block for oscillatory neural networks (ONNs).

In this work, we demonstrate the operation of individual VO<sub>2</sub> oscillators and their coupling dynamics, providing a foundation for their use in neuromorphic systems. Through experimental measurements, we validate the conditions required for stable oscillations in a single VO<sub>2</sub> oscillator and characterize the synchronization behavior of coupled oscillators. We analyze the influence of key circuit parameters on the transition between oscillatory and non-oscillatory states. Furthermore, we explore the synchronization dynamics of coupled VO<sub>2</sub> oscillators, identifying the mechanisms governing phase locking and asynchronous behavior to create oscillatory neural network. Although we have not yet fabricated a full oscillator network, we simulate its performance using data extracted from coupled oscillator experiments. These simulations confirm the potential of VO<sub>2</sub>-based oscillatory networks for neuromorphic computing applications, such as pattern recognition and edge detection.

Leveraging the phase dynamics of coupled VO<sub>2</sub> oscillators, we show their potential for spatial information processing, akin to biological neural systems. The results highlight the feasibility of using VO<sub>2</sub> oscillators for energy-efficient and hardware-friendly neuromorphic architectures.

## Epitaxial $(\text{Al}_x\text{Ga}_{1-x-y}\text{In}_y)_2\text{O}_3$ alloys lattice matched to monoclinic $\text{Ga}_2\text{O}_3$ substrates

Stephen Schaefer, Michelle Smeaton, Kingsley Egbo, Syed Hasan, William Callahan, Glenn Teeter, Andriy Zakutayev, and M. Brooks Teliepsky

<sup>1</sup>National Renewable Energy Laboratory, Golden, CO 80401, USA

Gallium oxide ( $\text{Ga}_2\text{O}_3$ ) is an emerging ultra-wide bandgap semiconductor material that has attracted attention for its potential to outperform existing SiC and GaN based devices operating at high breakdown voltages and high temperature. Isovalent alloying of In and Al in  $\beta\text{-Ga}_2\text{O}_3$  provides the ability to engineer bandgap energy and strain of the material. Alloying with Al increases the bandgap energy and the theoretically achievable Baliga's figure of merit, a key measure of a material's ultimate performance limits for high power switching devices. Alloying with In introduces compressive strain and can be used to counteract the tensile strain of Al incorporation. The resulting  $(\text{Al}_x\text{Ga}_{1-x-y}\text{In}_y)_2\text{O}_3$  alloy can be lattice-matched to commercially available  $\text{Ga}_2\text{O}_3$  wafers and has a tunable bandgap energy greater than that of  $\text{Ga}_2\text{O}_3$ , 4.76 eV. Such lattice-matched material can be grown arbitrarily thick without the detrimental effects of elastic strain and relaxation, making it suitable for high voltage diodes and transistors.

We have epitaxially stabilized a series of monoclinic  $(\text{Al}_x\text{Ga}_{1-x-y}\text{In}_y)_2\text{O}_3$  alloys by careful choice of molecular beam epitaxy growth conditions which balance alloy growth with suboxide desorption. The films are pseudomorphic to (010)  $\beta\text{-Ga}_2\text{O}_3$  substrates at thicknesses up to 150 nm with compositions ranging from  $(\text{Al}_{0.01}\text{Ga}_{0.83}\text{In}_{0.16})_2\text{O}_3$  to  $(\text{Al}_{0.24}\text{Ga}_{0.75}\text{In}_{0.03})_2\text{O}_3$ . The absorption edge shifts from approximately 4.62 eV to 5.14 eV with coincidentally increasing Al and decreasing In mole fractions. J-V measurements reveal an increase in resistivity over 4 orders of magnitude with a maximum value of  $4.2 \times 10^5 \text{ } \Omega\text{-cm}$  for  $(\text{Al}_{0.17}\text{Ga}_{0.76}\text{In}_{0.07})_2\text{O}_3$  which has nearly identical lattice parameters (both in-plane and out-of-plane) to the underlying  $\beta\text{-Ga}_2\text{O}_3$ . Scanning transmission electron microscopy of this sample reveals a mostly uniform and single crystalline film, though we identify areas of non-uniform In incorporation and some  $\gamma$ -phase inclusions. This work demonstrates the feasibility of thick layers lattice-matched to  $\beta\text{-Ga}_2\text{O}_3$  with increased band gap compared to phase-separation limited  $(\text{Al,Ga})_2\text{O}_3$ . These alloys can enable higher band gap epitaxial dielectrics and high sheet charge density transistors by increasing the conduction band offset with respect to  $\beta\text{-Ga}_2\text{O}_3$ .



# Understanding and Controlling the Atomic Structure at NiO/Ga<sub>2</sub>O<sub>3</sub> PN Junction Interface

Chris Chae<sup>1</sup>, Dong-Su Yu<sup>2</sup>, Hongping Zhao<sup>2</sup>, and **Jinwoo Hwang**<sup>1</sup>

1. Department of Materials Science and Engineering, The Ohio State University, Columbus OH 43210, USA
2. Department of Electrical and Computer Engineering, The Ohio State University, Columbus OH 43210, USA

## Abstract

This presentation discusses our recent electron microscopy study on the atomic structure and defects at the interface between p-type NiO and n-type  $\beta$ -Ga<sub>2</sub>O<sub>3</sub>. The NiO/Ga<sub>2</sub>O<sub>3</sub> interface has been investigated as a promising candidate for gallium oxide-based PN junctions. While the epitaxial growth of NiO on  $\beta$ -Ga<sub>2</sub>O<sub>3</sub> has been demonstrated using various growth methods, several important questions remain, including: (i) what determines the crystal orientation of NiO, (ii) what types of defects or intermediate layers form at the interface, (iii) how the interface structure is affected by the growth temperature, and (iv) how these factors influence the electrical properties of the interface. We conducted atomic-scale investigations using scanning transmission electron microscopy to reveal the detailed structure and defects at the NiO/Ga<sub>2</sub>O<sub>3</sub> interface, addressing the aforementioned questions. Our results show the formation of a cubic spinel NiGaO intermediate layer at the interface. The mechanism of NiGaO formation closely resembles the phase transition from  $\beta$ - to  $\gamma$ -phase Ga<sub>2</sub>O<sub>3</sub> (which is also a cubic spinel), as we previously reported. The thickness of the interface depends on the growth temperature. Importantly, in many cases, we found that the orientation of NiO is dependent on the formation of the interlayer, which effectively acts as a strain mitigator at the interface. We correlate the characteristics of this interlayer on the properties of the PN junction, such as leakage current and carrier mobility. Our findings provide a detailed understanding of the NiO/Ga<sub>2</sub>O<sub>3</sub> interface structure, which will aid in designing an optimized interface with desired properties.

# Physics Informed Neural Network for Predicting Characteristics of $\beta$ -Ga<sub>2</sub>O<sub>3</sub> based FETs.

Tasnia Jahan<sup>1</sup>, Kexin Li<sup>1</sup>

<sup>1</sup>School of Electrical, Computer and Energy Engineering,

Arizona State University, Tempe, AZ 85287, US

tjahan@asu.edu

Gallium oxide (Ga<sub>2</sub>O<sub>3</sub>), an emerging ultra-wide-bandgap semiconductor, has earned significant attention for high-temperature sensing, RF, and power applications. This is attributed to its ultra-wide bandgap of approximately 4.8 eV, the availability of large-diameter wafers, and exceptional thermal stability, surpassing that of Si, SiC, and GaN[1]. However, as an emerging material and device technology, Ga<sub>2</sub>O<sub>3</sub> electronics face significant challenges, including considerable non-uniformity in epitaxy and processing thermal management constraints. Unlike high-mobility systems such as AlGaN/GaN, the electron velocity and cutoff frequency ( $f_t$ ) in  $\beta$ -Ga<sub>2</sub>O<sub>3</sub> are influenced by a complex interplay of intrinsic and extrinsic device parameters, requiring meticulous optimization of these parameters[2]. Scanning and optimizing such an extensive device parameter space along with understanding optimal designs is essential to advancing this technology especially for enhancing logic and RF performance. Traditionally, TCAD has been employed to accurately model the complex nonlinear relationships between FET parameters—such as geometry, doping, bias, and the desired outputs. While effective for simpler architecture and a limited set of input parameters, this approach encounters challenges with advanced devices. The vast number of calculations needed to capture the complete physics of the input-output relationship makes the process highly time-intensive. This establishes Ga<sub>2</sub>O<sub>3</sub> devices as an ideal platform for implementing the TCAD-ML framework.

Though the data-driven neural network has shown promising accuracy, the method still has significant issues, including unphysical behaviors, such as nonzero drain current  $I_d$  at  $V_{ds}=0$ , and discontinuities in the derivatives of the current-voltage (I-V) curves [3]. Moreover, the ANN modeling method demands a substantial quantity of data as a training set to guarantee the model's fitting accuracy. To solve these issues, we will utilize a novel approach called Physics-informed neural network (PINN), in which the physics of the problem is incorporated into the NN, which is expected to improve predictability even outside the training dataset range. The ideal approach would involve training the model using data from real fabricated devices. However, the limited availability of experimental data necessitated an alternative solution. As a result, we will utilize TCAD simulations to generate the required training data. To develop a comprehensive deep learning model, we will incorporate a wide range of data from TCAD simulations, covering diverse input parameters such as gate length, oxide thickness, source/drain doping, gate work function, gate-source voltage and drain-source voltage. The simulations will output a rich dataset including current-voltage (I-V) characteristics, electrostatic potential ( $\phi$ ), electron density ( $n$ ), and net space

charge. We will also employ a deep learning model to analyze and predict DC characteristics, including gate capacitance, threshold voltage ( $V_{th}$ ), subthreshold swing (SS), on current ( $I_{on}$ ), and off current ( $I_{off}$ ). Our goal will be to use artificial neural networks to learn and adapt to unknown systems, approximate complex nonlinear relationships, and provide optimal results without the need for retraining.

- [1] S. J. Pearton *et al.*, “A review of Ga<sub>2</sub>O<sub>3</sub> materials, processing, and devices,” *Appl. Phys. Rev.*, vol. 5, no. 1, 2018.
- [2] H. Y. Wong *et al.*, “TCAD-Machine learning framework for device variation and operating temperature analysis with experimental demonstration,” *IEEE J. Electron Devices Soc.*, vol. 8, no. August, pp. 992–1000, 2020, doi: 10.1109/JEDS.2020.3024669.
- [3] W. Yang *et al.*, “A Physics-Informed Artificial Neural Network Modeling Approach for Wide Temperature Range 4H-SiC MOSFETs,” *ICSMD 2023 - Int. Conf. Sensing, Meas. Data Anal. Era Artif. Intell. Proc.*, pp. 1–4, 2023, doi: 10.1109/ICSMD60522.2023.10490903.

# Posters



Direct evidence for the 2-D Penrose tiling frame of 3-D quasicrystals.

Chung-Yuan Kung,

Department. of Electrical Engineering, National Chung Hsing University.  
145 Xingda Road., South Dist. Taichung City 40227. Taiwan. Telephone:  
886-4-22850359, E-mail Address: cykung@dragon.nchu.edu.tw.

## Abstract

Penrose tiling is 2-D geometric framework whose internal structure can change infinitely, whereas a quasicrystal is a 3-D phenomenon that reaching stability in growth but has not final yet stabilized. Penrose tiling is a mathematical problem of triangular geometry drawing, while quasicrystal HRTEM images are a physical problem that is inconsistent with the understanding of traditional crystal structures. The only correlation between the two problems is that they both have five-fold rotationally symmetric internal structures. How to prove that these two issues of different dimensions are correctly related to each other is a big problem that requires logical explanation.

In this study, a detailed analysis of high-resolution transparent electron microscopy (HRTEM) images of Al-Pd-Mn quasicrystals was performed, using color difference technology techniques to distinguish surface arrays of different characteristic atomic sites on the same image (comparing the size and position correlation of HRTEM and Penrose tiling atomic points as the first step of analysis). Four basic atomic clusters with five-fold mirror symmetry were identified, three of which can be regarded as nucleation centers that coarsening with the fourth atomic clusters respectively to form a larger atomic cluster, eventually showing coupled Penrose tiling characteristics.

The  $spd(f)3-d(4f)$  electronic sublevel filling model was used to explain the possible formation of van der Waals molecules, resulting in five-fold symmetric atomic clusters with weak van der Waals bond characteristics, and explaining the 3-D liquid behavior of quasicrystals.

A coupled Penrose tile diagram was created to point-to-point match to the atomic point array of the Al-Pd-Mn HRTEM photograph. Apparently, a Penrose tile framework (lattice) structure does exist in the

atomic array of a quasicrystal. A simple slanted-shift rotational stacking model is proposed to fabricate 3D (liquid) quasicrystals with relatively weak bonds between adjacent layers.

# Optimization of Optical and Electrical Properties of Doped ZnO Thin Films Using Machine Learning Models for Advanced Optoelectronic Applications

Ibrahima Niang<sup>1</sup>

<sup>1</sup>*Semiconductor and Solar Energy Laboratory of Senegal, Dakar*

<sup>1</sup>*Department of Physics, University Cheikh Anta DIOP of Dakar/Senegal*

[ibrahima35.niang@ucad.edu.sn](mailto:ibrahima35.niang@ucad.edu.sn) / [ibrahimanian25@gmail.com](mailto:ibrahimanian25@gmail.com)

## Abstract

This paper presents an innovative approach combining experimentation and Machine Learning modeling to optimize the optical and electrical properties of doped ZnO thin films. Dopants such as Aluminum (Al), Gallium (Ga), and others are used to enhance the electrical conductivity and optical transparency of the films, which are critical for optoelectronic devices such as light-emitting diodes (LEDs), solar cells, and sensors.

The study integrates advanced deposition techniques (e.g., sputtering, electron beam evaporation) with Machine Learning algorithms to:

1. Predict the performance of thin films based on fabrication parameters (temperature, dopant type and concentration, deposition conditions).
2. Identify optimal parameter combinations to maximize the desired properties.
3. Minimize experimental trial-and-error cycles through data-driven optimization.

The results will include a comparison of the performance of predictive models (neural networks, advanced regression, or random forests) and experimental validation on laboratory-produced samples. This work highlights a promising synergy between advanced materials and artificial intelligence, aligning with PACRIM and GOMD 2025 themes on ceramic and optical technologies.

## References:

- [1] D.Y Liu, L. Xu, Chip **1**, 100(2022).
- [2] Sh. J. Ikhamyies, N. M. Abu El-Haija, R. N. Ahmad-Bitar, PHYSICA SCRIPTA, **4**, 81 (2010)

# **Ionization of hydrogen, helium, beryllium, magnesium, and Zn by positron impact**

Jorge L S Lino

Instituto Lino, Departamento de Ciências Exatas,

12242000 São José dos Campos, São Paulo, Brazil.

## **Abstract**

This work describes the scaled Born positron (SBP) cross sections for the ionization of atoms (H, He, Be, Mg, and  $Z_n$ ) by positron impact. The same SBP method used for excitation electronic [1] is now tested for ionization cross sections for atoms by positron impact. The present study shows that at low, intermediate and high incident energies of incident positron the SBP method is consistent, indicating the possibility of rapid and reliable calculations of cross sections for applications in semiconductor. For the first time, ionization cross sections to these atoms are introduced within the SBP context. Where possible, our results are also compared to experimental data and computational approaches or in the absence of the results comparisons are made with analogous electron scattering.

[1]-Lino, J. L. S., Chin. J. Phys. 54 (2016) 223.

# Positive-Bias-Stress Instability, and Fast Trap Generation in AlGaIn/GaN HEMTs with Back Barrier during On-State Condition

Kevin Samways<sup>1</sup>, and Tae-Woo Kim<sup>1</sup>

<sup>1</sup>Department of Electrical and Computer Engineering, Texas Tech University, Texas

AlGaIn/GaN high-electron-mobility transistors (HEMTs) are promising candidates for high-power and RF applications due to their unique structure and superior material properties. However, device reliability remains a critical concern, mainly due to charge-trapping effects that degrade performance over time. Under ON-state stress conditions, electric fields at the AlGaIn/GaN interface can induce charge trapping, which is often attributed to the charging of preexisting, process-induced traps. Recent studies suggest prolonged stress may lead to additional trap generation, further exacerbating instability [1].

We conducted a series of on-state stress experiments to investigate these trapping effects on two GaN HEMT samples: Sample A (without a back barrier) and Sample B (with an AlGaIn back barrier). The devices, with dimensions  $L = 50 \mu\text{m}$  and  $W = 250 \text{ nm}$ , were subjected to  $V_{DS} = 5 \text{ V}$  stress for 1s, 5s, and 10s, followed by a three-minute relaxation period. This process was repeated for 15 cycles, with I-V characteristics measured between intervals to track threshold voltage shifts ( $\Delta V_T$ ).

Our results indicate rapid trap generation within a short stress duration ( $<10$  stress cycles). Furthermore, the presence of an AlGaIn back barrier significantly alters the trapping dynamics, suggesting a reduction in electron carrier capture. Pre- and post-stress I-V measurements reveal a clear  $\Delta V_T$ , further supporting the hypothesis that back-barrier engineering influences charge-trapping behavior. Understanding these mechanisms is crucial for optimizing GaN HEMT performance and long-term reliability.

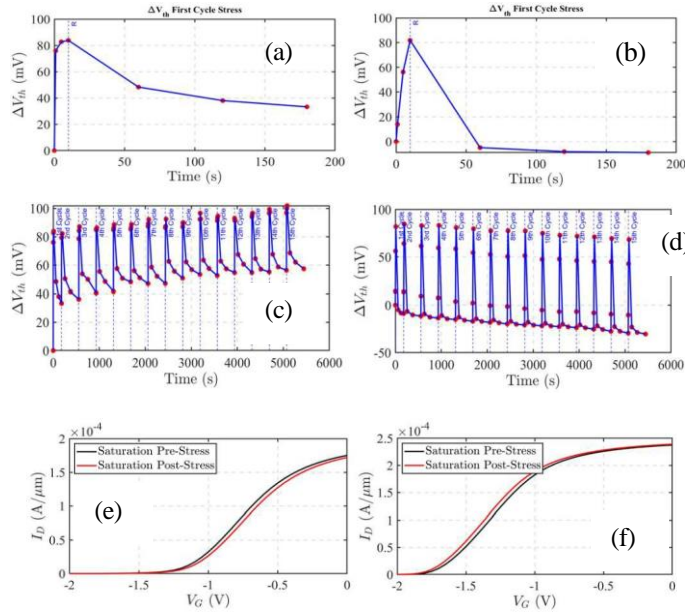


**Figure 1:** (a) Threshold voltage shift during first stress and relaxation cycle sample A. Relaxation begins at “R”. (b) Threshold voltage shift during first stress and relaxation cycle sample B. (c)  $\Delta V_T$  vs time for all cycles sample A. (d)  $\Delta V_T$  vs time for all cycles sample B. (e) Pre and post stress IV characteristics sample A. (f) Pre and post stress IV characteristics sample B.

**References** [1] Dimitris P. Ioannou et al, Microelectronics Reliability, vol. 54, issue 8, pp. 1489-1499, 2014.

# Material Quality Assessment of IGZO via Computer Vision-Assisted Conductive Atomic Force Microscopy

Md Jayed Hossain<sup>1</sup>, Filippo Ozino Caligaris<sup>1</sup>, Manuel Roldan Gutierrez<sup>2</sup>, and Umberto Celano<sup>1</sup>

<sup>1</sup> Arizona State University, School of Electrical, Computer, and Energy Engineering, Tempe AZ, 85281

<sup>2</sup> Eyring Materials Center Arizona State University, Tempe AZ, 85281

**Abstract:** Indium-Gallium-Zinc Oxide (IGZO) is a promising n-type semiconductor oxide, renowned for its exceptional electrical and mechanical properties, including high mobility, wide bandgap that enables transparency, as well as excellent electrical stability and flexibility. Consequently, it is emerging as a strong candidate for multiple applications including display technology, back-end-of-the-line (BEOL) compatible logic, and memories, thanks to its low thermal budget and compatibility with CMOS architecture. However, being a ternary alloy IGZO has a rich multitude of phases, and a major challenge lies in the costly and complex characterization for the material screening and process control. In this work, we report on the use of conductive atomic force microscopy (C-AFM), a powerful technique for the rapid screening of electrical properties of blanket IGZO films. This is enabled by the application of computer vision algorithms to classic C-AFM data acquisition. The results indicate that major material parameters can be extracted automatically, while maintaining nanometric resolution for the electrical features. Finally, we leveraged the power of computer vision and automation offered by Python scripting to analyze the results obtained from the raw C-AFM images, enabling accurate and automated assessment of IGZO samples. This approach allowed us to extract key parameters such as conductive spots, highly conductive areas, coverage percentage, and average current on the sample surface.

# **Z-scheme heterojunction g-C<sub>3</sub>N<sub>4</sub>/Bi<sub>2</sub>WO<sub>6</sub> highly efficient degradation of levofloxacin: Performance, mechanism and degradation pathway**

Menglan Wei

## **Abstract:**

g-C<sub>3</sub>N<sub>4</sub>/Bi<sub>2</sub>WO<sub>6</sub> (MCN/BWO) heterojunction photocatalysts were synthesized via one-step hydrothermal method for levofloxacin (LEV) degradation. The MCN/BWO (1:1) exhibited 98.14% removal efficiency for 15 mg/L LEV and its pseudo-first-order reaction rate constants were 2.58, 1.18, 1.42 and 1.80 times higher than those of MCN, BWO, MCN/BWO (1:3), and MCN/BWO (3:1), respectively. The toxicity prediction and experimental findings indicated that the toxicity of the degraded LEV solution was notably diminished. The MCN/BWO catalyst exhibited high reusability and stability. Outstanding photocatalytic performance of MCN/BWO photocatalyst is primarily due to the successful formation of Z-scheme heterostructure that generate more  $\cdot\text{O}_2^-$  and  $\text{h}^+$  to degrade LEV. Furthermore, measurements of photoluminescence spectrum, electrochemical impedance spectroscopy, transient photocurrent and surface photovoltage confirmed the fast electron-hole separation and slow charge recombination in MCN/BWO, thereby boosting the photocatalytic efficiency. Finally, in conjunction with a diverse range of experimental methodologies, the degradation pathway of LEV through the MCN/BWO composite catalyst and the electron transfer mechanism within the Z-scheme heterojunction have been comprehensively elucidated. This study provides a pioneering reference for optimizing g-C<sub>3</sub>N<sub>4</sub>-based heterojunction catalysts and addressing antibiotic-contaminated wastewater treatment.

**Keywords:** Z-scheme heterojunction; MCN/BWO; photocatalysis; levofloxacin; degradation pathway

# Ultrasound Action on Radiation Defects at the Silicon Dioxide / Silicon Interface of MOS Structure

Oleg Olikh\*, Alla Gorb, Oleg Korotchenkov, Artem Podolian, and Roman Chupryna  
 Department of General Physics, Taras Shevchenko National University of Kyiv, Kyiv, Ukraine

\*email: [olegolikh@knu.ua](mailto:olegolikh@knu.ua)

It is widely recognized that ultrasound can serve as an effective tool for influencing defects in semiconductors. Similar effects have been observed in Si/SiO<sub>2</sub> structures [1]. This study presents the results of acoustically induced annealing of radiation defects in  $\gamma$ -irradiated silicon MOS structures.

The experiments revealed that gamma irradiation (<sup>60</sup>Co source,  $5 \cdot 10^7$  rad) of Au-SiO<sub>2</sub>-Si structures alters the current mechanism under low bias conditions (<1 V) (see Fig. 1a). In the pristine structures, thermionic emission (TE) over the potential barrier was the dominant process. However, after irradiation, the  $I$ - $V$  characteristics align with a power-law behavior. A slope value of  $\sim 1.3$  suggests the presence of space-charge-limited current with an exponential distribution of trap density. In this context [2]:

$$I = Aq^{l-1}\mu N_c \left( \frac{2l+1}{l+1} \right)^{l+1} \left( \frac{l}{l+1} \frac{\epsilon\epsilon_0}{N_t} \right)^l \frac{V^{l+1}}{d^{2l+1}} = R_{SCLC} \cdot V^{l+1}, \quad (1)$$

where  $N_t$  is the density of traps,  $l$  is the parameter given by  $l = E_c / kT$  and  $E_c$  is the characteristic energy of traps distribution. The activation energy (0.32 eV), determined from the temperature dependence of the current, suggests that the primary SCLC defects are Pb centers.

Ultrasound treatment (4 MHz, 2 W/cm<sup>2</sup>, room temperature) of the irradiated MOS structures was performed using two consecutive loading-unloading cycles, each lasting 30 minutes. The total treatment time was either 30 minutes (UST30) or 60 minutes (UST60). Under the influence of ultrasound, an increase in  $l$  (broadening of the trap energy distribution) and a decrease in  $R_{SCLC}$  (reduction in the trap total concentration  $N_t$ ) were observed. Analysis of the reverse current showed that UST also reduces the concentration of E' centers, which actively participate in trap-assisted tunneling processes. In our opinion, the observed defect annealing can be attributed to the acoustically stimulated diffusion of interstitial oxygen and hydrogen atoms.

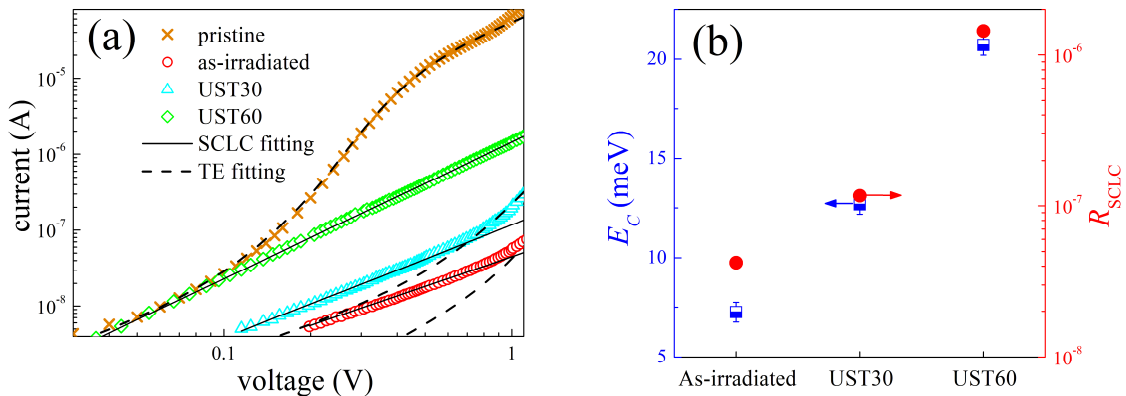


Figure 1: (a) Current versus forward bias voltage for MOS silicon structure. The marks are the experimental results, and the solid and dashed lines are the SCLC and TE fitted curves. (b) UST influence on SCLC characteristics.

- [1] D. Kropman, V. Seeman, S. Dolgov and A. Medvids, Phys. Status Solidi C 13, 793 (2016).
- [2] S. Kazmi *et al.*, Physica B 670, 415400 (2023).
- [3] P. K. Hurley *et al.*, J. Appl. Phys. 93, 3971 (2003).



**Structurally Modulated NiV-LDH with CdMoSe-Quantum Dot: Unlocking the active centers at S-scheme heterojunction for stimulating Photocatalytic H<sub>2</sub>O<sub>2</sub> production and H<sub>2</sub> evolution**

**Preeti Prabha Sarangi<sup>1</sup>, Kulamani Parida<sup>1\*</sup>**

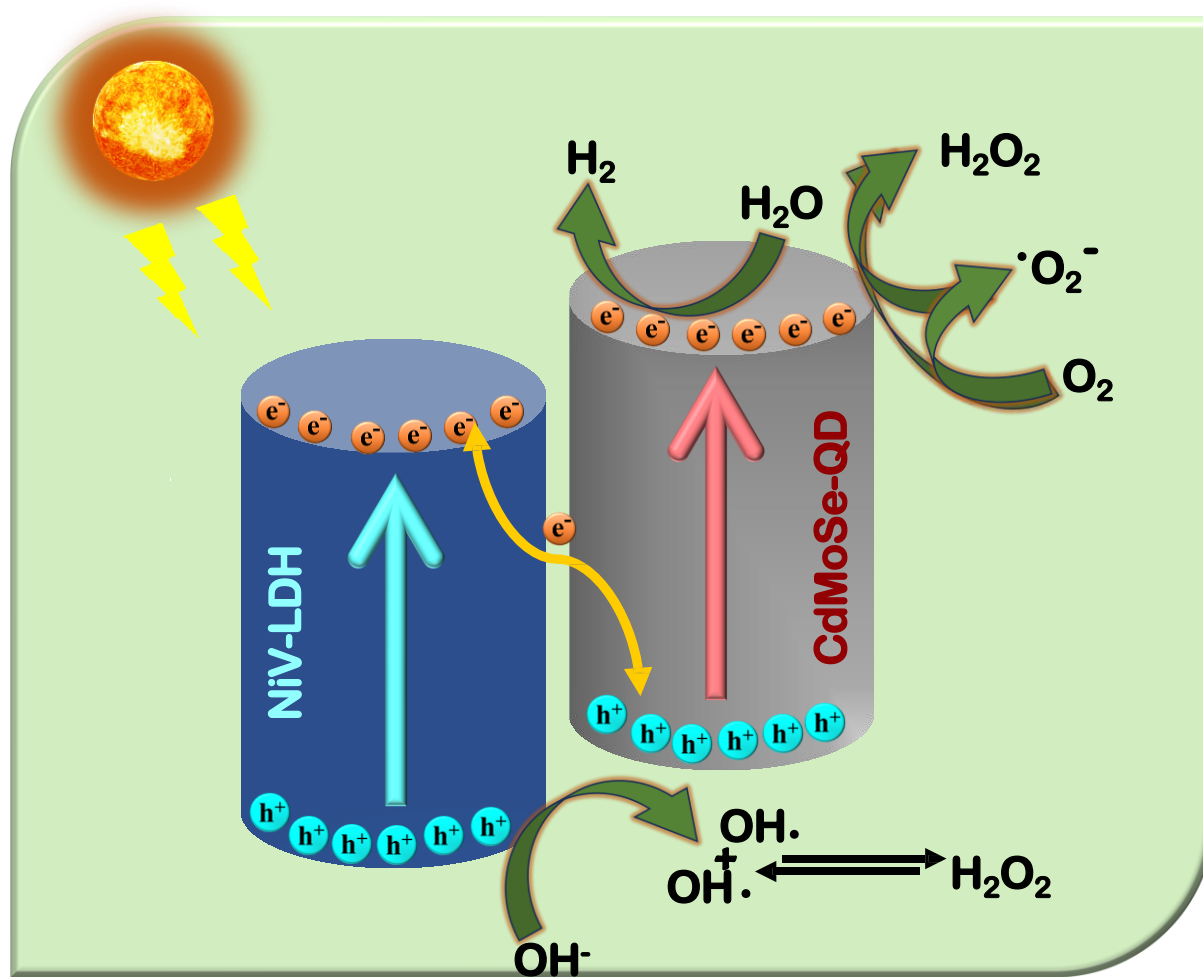
<sup>1</sup>*Centre for Nanoscience and Nanotechnology, SOA (Deemed to be University), Khandagiri, Bhubaneswar, Odisha, India*

\*Presenter E-mail: sarangipreetiprabha9178@gmail.com

**ABSTRACT**

Efficient photocatalytic production of H<sub>2</sub>O<sub>2</sub> and H<sub>2</sub> from water is a cost-effective and sustainable way to address the environment and energy crisis. Therefore, developing a high performing photocatalyst is highly essential for present need. The fabrication of a constructive heterostructure and thus the induced 0D/2D interfacial phase indicates great importance in semiconductor based photocatalysts. Herein, a novel S-scheme heterojunction photocatalyst CdMoSe quantum dots/NiV-LDH (CNV) is fabricated through in-situ reflux method. The optimal photocatalyst i.e. CNV-1 presents an outstanding H<sub>2</sub>O<sub>2</sub> production rate of 1867.9  $\mu\text{mol g}^{-1} \text{h}^{-1}$  which is about 3 and 1.6 times higher than that of pristine NiV-LDH and CdMoSe quantum dots. Similarly, the CNV-1 displays H<sub>2</sub> generation rate of 981.2  $\mu\text{mol g}^{-1} \text{h}^{-1}$  which is 5.2 and 6.2 times than that of pristine NiV-LDH and CdMoSe quantum dots respectively. The enhanced photocatalytic activity is attributed to the mutual effect of enhanced photon absorption properties and promoted charge segregation and migration induced by S-scheme heterojunction. Moreover, the delayed recombination of charge carriers was well supported by PL, EIS and TPC measurements. The S-scheme charge-migration path was well confirmed from work-functions evaluated from UPS measurement, active species trapping experiment, terephthalic acid (TA), nitro blue tetrazolium chloride (NBT), and EPR analysis.

**Keywords:** S-scheme, photocatalysis, H<sub>2</sub>O<sub>2</sub> generation, H<sub>2</sub> generation



**Scheme1.** Schematic representation of photocatalytic  $\text{H}_2\text{O}_2$  generation and  $\text{H}_2$  evolution

# Influence of polarity on electrical properties of CuI/ZnO heterojunctions

R. Yatskiv<sup>1</sup>, S. Tiagulskyi<sup>1</sup>, J. Grym<sup>1</sup>, S. A. Irimiciuc<sup>2</sup>, J. Lancok<sup>2</sup>

<sup>1</sup>Institute of Photonics and Electronics of the Czech Academy of Sciences, Czech Republic

<sup>2</sup>Institute of Physics of the Czech Academy of Sciences, Czech Republic

E-mail address: [yatskiv@ufe.cz](mailto:yatskiv@ufe.cz)

Transparent electronics represents a rapidly evolving field of research with numerous applications, including solar cells, photodetectors, thermoelectric devices, and flat panel displays. The utilization of wide-bandgap semiconductors, such as CuI and ZnO, in transparent electronics demonstrates considerable potential. The quality of the interface between CuI and ZnO is determined by various factors, and is crucial for the fabrication of high-quality heterojunctions. This study examines how surface polarity in ZnO influences interface quality in such heterojunctions. It is experimentally demonstrated that distinct interactions between CuI and the O- or Zn-polar face of ZnO induce the uneven development of interface imperfections. CuI deposition on the Zn face of bulk ZnO and ZnO nanorods results in a lower quality heterojunction with a reduced rectification ratio and an increased ideality factor. Conversely, a lower density of states is observed for the O face, which is reflected in the decreased ideality factor and enhanced rectification ratio for the CuI/ZnO heterojunction.

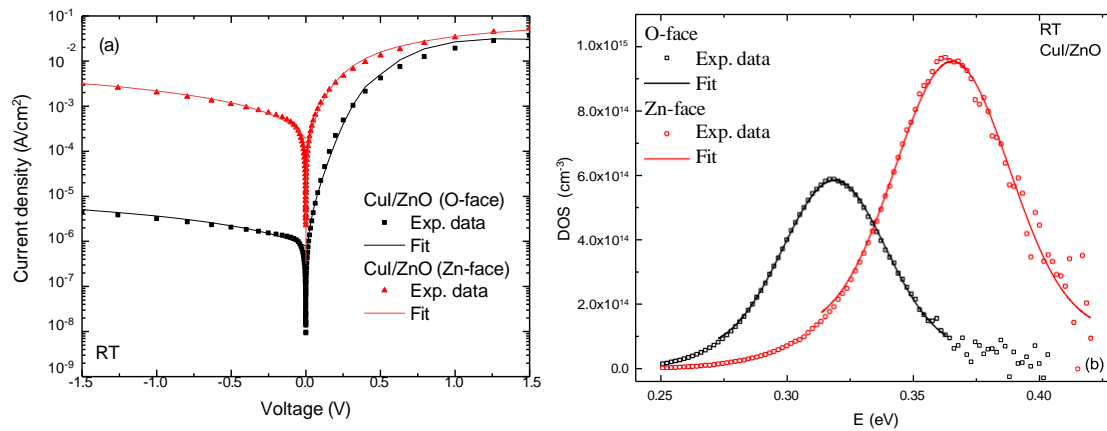


**Fig. 1** (a) a representative room temperature I–V characteristics and (b) DOS distributions of CuI/ZnO heterojunction fabricated on O-and Zn-face ZnO substrate.

# **Porosity increases in radio frequency sputtered TeO<sub>2</sub> films investigated by variable-energy positron annihilation spectroscopy.**

T. Wu, J.M. Gaudet, J.D.B. Bradley, A.P. Knights, and P. Mascher  
Department of Engineering Physics, McMaster University, Hamilton, Canada

Keywords: TeO<sub>2</sub>, Positron Annihilation Spectroscopy, Porosity

Tellurium Oxide is an interesting semiconductor material as it has both amorphous and crystalline forms. Such characteristics indicate its potential in multiple applications such as  $\gamma$  ray detectors and gas sensors [1]. Its unique optical properties such as transparency throughout the visible and mid infrared with low dispersion makes it a promising material in optical waveguides [2][3]. However, defects in RF sputtered material usually hinder device performance through increased waveguide losses [2]. Thus, it is important to study defects in such films, and Doppler Broadening Positron Annihilation Spectroscopy (DBPAS) is a perfect tool for studying microscopic scale vacancies, voids, and pores.

A set of TeO<sub>2</sub> on silicon substrates samples with different annealing temperatures up to 415 °C were scanned by the McMaster variable energy positron beam with different acceleration potentials. All results were fitted by a 4 layer model in the positron fitting tool VEPFIT. We assume the first 3 layers to be TeO<sub>2</sub> with different thicknesses and positron diffusion length and the 4<sup>th</sup> one the silicon substrate. We observed an S parameter peak forming at the second layer at a depth of around 70nm for samples that were annealed below 400°C. Combining the R parameter (3  $\gamma$  o Ps annihilation parameter) which also gives a plateau at the same depth and results from a previous study [4], we suspect the second layer which has an increase in S parameter representing the porosity of the film, and such a layer is expanding with increasing annealing temperature.

- [1] Dewan, N., Sreenivas, K., & Gupta, V. (2008). Comparative study on TeO<sub>2</sub> and TeO<sub>3</sub> thin film for  $\gamma$  ray sensor application. *Sensors and Actuators A: Physical*, 147(1), 115-120.
- [2] Miarabbas Kiani, K., Bonneville, D. B., Knights, A. P., & Bradley, J. D. (2022). High Q TeO<sub>2</sub>-Si hybrid microring resonators. *Applied Sciences*, 12(3), 1363.
- [3] Frankis, H. C., Kiani, K. M., Bonneville, D. B., Zhang, C., Norris, S., Mateman, R., ... & Bradley, J. D. (2019). Low loss TeO<sub>2</sub> coated Si<sub>3</sub>N<sub>4</sub> waveguides for application in photonic integrated circuits. *Optics Express*, 27(9), 12529-12540.
- [4] Siciliano, T., Di Giulio, M., Tepore, M., Filippo, E., Micocci, G., & Tepore, A. (2010). Effect of thermal annealing time on optical and structural properties of TeO<sub>2</sub> thin films. *Vacuum*, 84(7), 935-939.

**Fei Teng**

**Degradation of Tetracycline with g-C<sub>3</sub>N<sub>4</sub>/BiVO<sub>4</sub> Modified by Carbon  
Quantum Dots Derived from Peanut Shells**

**ABSTRACT**

g-C<sub>3</sub>N<sub>4</sub>/BiVO<sub>4</sub> modified with carbon quantum dots (CQDs) was synthesized via a hydrothermal method. The catalyst was characterized and analyzed using SEM, XRD, DRS, TPC, EIS, and M-S techniques. Under xenon lamp irradiation, the degradation rate of tetracycline by the CQDs/g-C<sub>3</sub>N<sub>4</sub>/BiVO<sub>4</sub> (pCQDsCNB) reached 90.5%, which is 1.54 times and 1.22 times that of BiVO<sub>4</sub> and g-C<sub>3</sub>N<sub>4</sub>, respectively. ·O<sub>2</sub><sup>-</sup>, h<sup>+</sup> and ·OH play significant roles in the photodegradation process. Utilizing the transfer of photogenerated electrons from the conduction band of g-C<sub>3</sub>N<sub>4</sub> to CQDs, efficient separation of photogenerated electrons in CQDs was achieved, thereby significantly enhancing the photocatalytic activity of pCQDsCNB.

pCQDsCNB composite material demonstrates higher photocatalytic activity compared to g-C<sub>3</sub>N<sub>4</sub> and BiVO<sub>4</sub>. After complexation, the morphological characteristics of BiVO<sub>4</sub> changed significantly, with BiVO<sub>4</sub> evenly distributed on g-C<sub>3</sub>N<sub>4</sub> and CQDs dispersed between g-C<sub>3</sub>N<sub>4</sub> and BiVO<sub>4</sub>, resulting in smaller particle size and increased contact area between the antibiotic and the catalyst. Under xenon lamp irradiation for 240 min, the degradation efficiency of 10 mg/L TC by pCQDsCNB composite material reached 90.5%, which is 1.54 times that of BiVO<sub>4</sub> and 1.22 times that of g-C<sub>3</sub>N<sub>4</sub>. Through active species analysis, pCQDsCNB exhibits a higher charge transfer rate, capable of generating more h<sup>+</sup>, ·O<sub>2</sub><sup>-</sup> and ·OH to degrade TC.

## **Study on the performance of CeVO<sub>4</sub>/InVO<sub>4</sub> composite catalyst for photodegradation of levofloxacin**

Yimeng Wang

CeVO<sub>4</sub>/InVO<sub>4</sub> composite materials were prepared by the hydrothermal method, with the molar ratios of CeVO<sub>4</sub> to InVO<sub>4</sub> being 1:0, 1:1, 2:1, 4:1, and 0:1, respectively. The crystal structure, morphology, microstructure and optical properties of the CeVO<sub>4</sub>/InVO<sub>4</sub> composite photocatalysts were characterized by X-ray diffraction (XRD), scanning electron microscopy (SEM), Fourier transform infrared spectroscopy (FTIR) and ultraviolet-visible diffuse reflectance spectroscopy (DRS). Under visible light irradiation, the photocatalytic activity was evaluated by the degradation of levofloxacin (LEV). The results showed that pure InVO<sub>4</sub> as a photocatalyst degraded about 32.0% of levofloxacin in 3 h of visible light irradiation, while pure CeVO<sub>4</sub> as a photocatalyst only degraded about 24.6% of levofloxacin. Due to the improved separation and transfer efficiency of photogenerated electron-hole pairs, CeVO<sub>4</sub>/InVO<sub>4</sub> (1:1, 2:1, 4:1) samples degraded about 41.4%, 58.2%, and 91.1% of levofloxacin, respectively, confirming that the photocatalytic activity of CeVO<sub>4</sub>/InVO<sub>4</sub> heterojunction composite materials towards levofloxacin is superior to that of pure InVO<sub>4</sub> and CeVO<sub>4</sub>. Among the composite photocatalysts, the CeVO<sub>4</sub>/InVO<sub>4</sub> composite photocatalyst with a molar ratio of 4:1 exhibited the best photocatalytic performance. The apparent rate constant of the best photodegradation of LEV under xenon lamp was 0.01172 min<sup>-1</sup>, which was 3.3 times and 2.1 times that of the 1:1 and 2:1 catalysts, respectively. The excellent photocatalytic performance of the CeVO<sub>4</sub>/InVO<sub>4</sub> composite photocatalyst is attributed to the efficient migration and separation of carriers and enhanced light absorption ability. This study provides a promising approach for the design and development of visible light-responsive photocatalysts for antibiotic wastewater treatment.